RSC Advances

ROYAL SOCIETY OF CHEMISTRY

www.rsc.org/advances

RSC Advances RSCPublishing

REVIEW

Isoindoline-Derived Ligands and Applications

Cite this: DOI: 10.1039/x0xx00000x

Received 00th January 2012,
Accepted 00th January 2012

DOI: 10.1039/x0xx00000x

www.rsc.org/

Róbert Csonka, Gábor Speier and József Kaizer*

During the past decade isoindoline-based ligands became subject of growing interest due to their modular set-up. In this review the structure and reactivity of these ligands and their transition metal complexes are covered. Beyond the discussion of the structural properties particular attention is paid to the expanding fields of applications of these compounds.

1. Introduction

The first tridentate bis(arylimino)isoindoline type ligand with N,N,N binding mode was introduced in the early 1950s by Elvidge and Linstead.[1,2] Although, it was clear from the beginning that this compound family can act as potent metal chelators their coordination chemistry started to make a considerable progress from the late 1970s and 1980s.[3-5] At this time the first X-ray structure was published[6] and also alternatives for ligand synthesis.[7] Concerning the possible starting materials diiminoisoindoline (DII or **2**) and phthalocyanines, they have been utilized as building blocks of supramolecular architectures in their metal complex form,[8] and optical properties have been researched and exploited as well.[9] The tunability of the parent materials creates a wide variety of bi- and tridentate ligands. Some *in vitro* biological tests showed that by small modifications on the isoindole base antiproliferative activity can be achieved even without the presence of any metals,[10] furthermore isoindoline carbamates have a structural key role in diuretic or blood pressure regulator agents.[11,12] By the application of chiral sidearm enantioselective catalysis can be carried out[13] that is important both in industrial and medicinal chemistry.

The main structural features involve bis(arylimino), bis(alkylimino) and monosubstituted (asymmetric) isoindolines. Another structure of interest belongs to the phthalazine type molecules originated from bis(R-imino)isoindolines (BII or **3**) by ring expansion with hydrazine hydrate.[14] The transition metal complexes of these formulations have applications from enzyme mimics[15-17] to catalytic hydrogenation[18] or in photophysics,[19] that is discussed in this review.

2. Synthetic routes, characteristics

2.1. In solution synthesis

The more than six decades long history of bis(R-imino)isoindolines (**3**) synthesis created two main methods that are generally followed by scientists (Scheme 1). The applicability of these methods was partly reviewed by Tamgho *et al*. recently.[20] Fifteen old and new BII ligands, containing no other heteroatoms, were examined in their work and the original synthetic method[1] is compared to the more recent Siegl's method.[3] It was pointed out that the latter is a more suitable way of producing bulky and cyclic derivatives. According to the Linstead method phthalonitrile (**1**) has to be converted to 1,3-diiminoisoindoline (**2**) first (it is commercially available nowadays) then the imine condenses with amines in ethanol during a 24 hour reflux time. In Siegl's method phthalonitrile is directly used in a condensation reaction in the presence of $CaCl_2$. The reaction time is considerably long (usually 48 hours) but yields are higher.

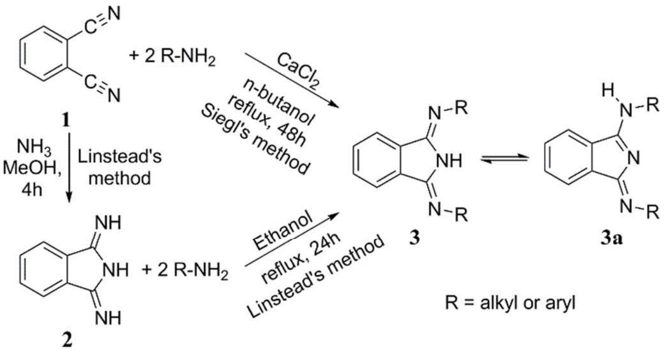

Scheme 1. Synthetic solutions resulting in BIIs

2.2. Fusion synthesis

The least used method at the synthesis of **3** is the fusion reaction of phthalonitrile **1** with primary amines at high temperature (180-190°C). Seemingly, it is a modification of the Siegl method but there are considerable advantages, namely it requires no solvent and reaction time is shorter (average 18 hours), while yields are above 80%.[21,22] The expected yield of the previous methods is 50-80%.

2.3. Structure based classification

A nice variety of derivatives have been created from **1** and **2**. The major groups of these compounds can be named based on the structure: aliphatic BII (aliBII),[20] aromatic BII (aroBII),[1] unsymmetrical BII (unsyBII),[23] chiral BII (chiBII)[13] and aminophthalazines (PAPs)[14] (Fig. 1). Phthalocyanines or subporphyrines are the cyclic formulations of DII but their synthesis requires different strategy from the previously mentioned molecules, furthermore their applications and research are both well documented.[24,25]

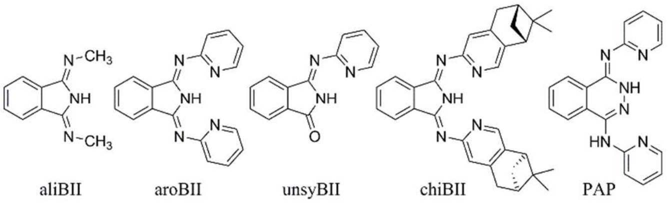

Fig. 1. Representatives examples of bis(R-imino)isoindoline subgroups

By the presence of aliphatic moieties on BII the chelating capacity is usually limited. The lack of heteroatoms favors the mono-, or bidentate ligand formation that is based on the coordination to the endocyclic NH and one imino side arm on the isoindole ring. Although, aliBIIs have been reported since the first appearance of BIIs,[2,20,26-31, 54] complexes of this kind have been synthesized only once by Maleev *et al*. In this work, the coordination of bidentate aliBII to rare earth metals is discussed. They are observed both in terminal and bridge positions using all three coordination sites in the latter case.[32]

The less common monodentate behavior of BII has been detected by our group[33] by blocking the N atoms of 1,3-bis(2´-pyridylimino)isoindoline – BPI (**7**). The zwitterionic copper(I) compound showed moderate catechol oxidase activity.

BPI and its substituted derivatives are the most researched aroBIIs. They are considered pincer type ligands based on the tridentate coordination mode and the aromatic planarity around the metal ions. They are monoanionic, nevertheless complexes of protonated ligands can form as well with suitable metal ions and the proper conditions applied.[34] The meridional configuration is open enough to host other coligands or various substrates. A second identical ligand stabilizes the structure creating an octahedral, homoleptic complex, although the active species remains usually the 1:1 ligand to metal ratio form.

Because of the favorable characteristics of BPI chiral side chains can be attached as well. Fletcher et al. reported a facile one pot synthesis of chiral aminopyridines.[35] To obtain any optically active BII is only one step away. Myrtene, α-pinene and carene have been used to build chiBIIs. Concerning enantioselective catalysis only a few number of work can be found done by Bröring and Gade.[13, 36-38]

The preparation of BIIs by all known methods is a two-step procedure. The partial condensation of the starting material might happen if reaction time is not adequate. This can be used to our advantage if the goal is to achieve unsyBII. Since intramolecular C-H bond activation has been observed multiple times by Pd complexes,[39-41] a better understanding on the mechanism is greatly expected. In order to study this phenomenon several unsyBIIs have been synthesized.[42,43] Unsymmetry have been proved to be useful in the research of catecholase activity as well.[23]

Versatility of BPI goes beyond its applications and side chain variations. Simply, by the addition of hydrazine hydrate a ring expansion occurs on the isoindoline core that reveals an entirely new chemistry (Scheme 2).[14]

PAP (**4**) has a similar behavior to **3**. It is anionic and it can form any metal complexes both in protonated or deprotonated state. Acetato, hydroxo, oxo, chloro *etc*. bridges are often observed in the binuclear center. The number of coordinated anions represented by L on Scheme 2 can vary depending on the metal salt used.

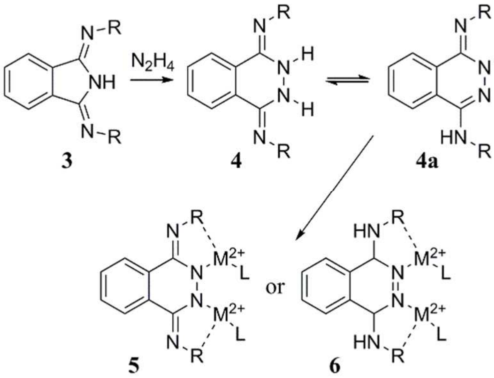

Scheme 2. Fluxionality of PAP ligands and complexes

In Figure 2 ligands have been collected that are the derivatives of both **3** and **4** showing only the R-group and their reference number used in this review.

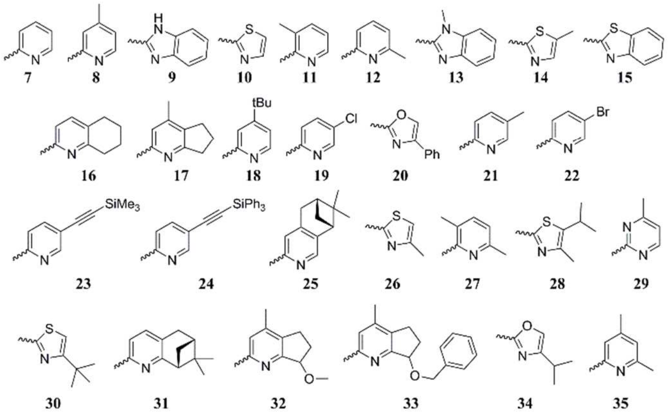

Fig. 2. R-groups of BII and PAP ligands

2.4. Characterization

The two imino moieties on the isoindole core have a strong impact on the planar structure of both BII and its coordination complexes. The double bond between N and C atoms extends aromaticity and increases the rigidity of the system. It can easily be detected by FT-IR and a characteristic NMR signs can be attributed to one of these arms when mostly aliphatic residues are attached to the BII.[20]

The second key structural element is the endocyclic NH group. It is responsible for an anionic character observed with metal ions. Depending on the electronic strength of R-groups, the anion applied with the metal ion, the solvent used, the inert atmosphere and the presence of bases both deprotonated and protonated complexes can be formed.

2.4.1. Crystallographic information

Although, numerous isoindoline derivatives have been reported not all of their complexes could be resolved by X-ray spectroscopy due to solubility and stability issues. The N,N,N binding mode (except for the Pd complexes where C,N,N binding is observed too – discussed later) appears in a trigonal bipyramidal (*TBPY-5*) structural arrangement characteristically at single complexes and octahedral (*OC-6*) symmetry point group materializes mostly at homoleptic formulations. At *TBPY-5*, the free coordination spots are filled by anions, coligands and solvent molecules. A special angular parameter τ has been devised to describe trigonality.[44] Usually, it is determined in percentage or a number between 0 and 1. The value expresses the extent of distortion from square pyramidal to trigonal bipyramidal. It can be useful in the search for ideal conditions in catalysis and synthesis.[45] A similar factor (tetrahedricity factor) has been suggested for tetrahedral/square planar complexes by Pap *et al*.[46] Certain structures balance on the borderline between these two alignments. The factor is a distortion degree that merely defines a four-coordinate complex based on the angle between all opposite L-M-L planes (Scheme 3). As Φ is approaching zero square planar structural features become dominant. By definition $\Phi = 0.5\ (\phi_1+\phi_2)/\phi_0$.

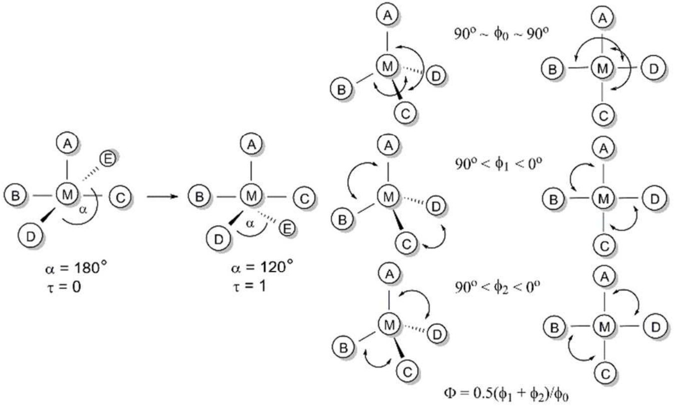

Scheme 3. The τ parameter (left) and tetrahedricity (Φ) (right)

2.4.2. Vibrational analysis, UV-Vis spectroscopy

It is general knowledge that FT-IR or UV-Vis cannot give enough information on complicated structures. However, for BIIs there are some characteristics that make identification simple. The H atom, that is responsible for the anionic character, is greatly mobile. Due to the aromaticity its possible positions are on one of the imino arms, or at the endocyclic amino group. In IR spectra the nonspecific $\nu_{C=N}$ vibrations modes that are mostly influenced by this proton appear as two very strong bands in the 1600 cm^{-1} to 1660 cm^{-1} interval in the free ligands. These bands are suppressed if coordination happens by deprotonation. In this case they shift below 1600 cm^{-1} loosing intensity at the same time. In case of nondeprotonated complexation the strong vibrations above 1600 cm^{-1} remain visible and additionally other intense bands appear around 1550 cm^{-1}.[34,46,74]
The electronic absorption spectrum of the ligands **3** show a multiple band pattern. The π-π* transitions are created by the extended π-bond system and they appear in the 360-500 nm region. Upon complex formation small (2-20 nm) red or blue shifts are observed. Lower energy bands are contributed to charge transfer transitions from metal ion to the ligand. A selection of absorption bands of various BII and their homoleptic transition metal complexes has been collected in Table 1.

2.4.3. NMR spectroscopy

Although, BII formation can be validated by IR and UV-Vis, the ultimate proof is NMR. In case if Linstead's method[1] is followed during synthesis the disappearance of the broad NH proton signs of **2** around 8.6 ppm (three protons due to delocalization) is an information on ligand formation. It has to be noted here, that the NH (either endocyclic or imino NH) appears beyond 12 ppm and sometimes it shifts out of the standard limits (14 ppm) of NMR instruments.[54] As it is expected from EDG groups on aromatic molecules a sufficient upfield shift can be detected (~11.5 ppm) while substituted pyridines can cause major downfield shifts (~14.0 ppm). The sign is hardly detectable because of its broadness and low intensity. The fluxional behavior is known of this proton that was documented by Tamgho *et al*. Aliphatic R-groups on **3** seem to place the proton to the imine location that was proved by multiplicity change from singlet to triplet by decreasing the temperature from 30°C to -50°C showing the interaction between NH and aliphatic CH_2.[20]

Table 1.
UV-Vis spectroscopic data of selected BII ligands and their complexes

Ligand	π–π* CT bands of the free ligands λ_{max}/nm (log ε)	$[M(L)_2]$ λ_{max}/nm (log ε) in DMF, (**metal complex**)	Reference
7	410 (3.99), 386 (4.23), 366 (4.19) in DMF	440 (4.58), 410 (4.81), 390 (4.75) (**Fe^{II}**)	[1]^a, [48]^b, [22]^c
8	408 (4.11), 385 (4.29), 366 (4.24) in DMF	450 (4.65), 423 (4.73), 332 (4.45), 306 (4.53) (**Mn^{II}**)	[1]^a, [49]^b, [22, 49]^c
9	470 (4.01), 440 (4.30), 413 (4.31), 388 (4.35), 369 (4.37) in DMF	493 (4.28), 453, (4.49), 389 (4.40), 367 (4.45) (**Fe^{II}**)	[50]^a, [22, 51]^{b,c}
		474 (4.71), 440 (4.86), 414 (4.86), 364 (4.94), 287 (4.87) (**Fe^{III}**)	
10	485 (3.18), 448 (3.86), 420 (4.05), 396 (4.01), 374 (3.94) in DMF	476 (4.11), 433 (4.54), 410 (4.55), 333 (4.38), 319 (4.40), 286 (4.45) (**Co^{II}**)	[52]^a, [53]^b, [22, 53]^c

^{a} ligand synthesis, ^{b} complex synthesis and X-ray, ^{c} spectroscopic data

3. Transition metal complexes of BII ligands

Structural and spectroscopic features of BII have been collected in details up to this point. The second part of this review will focus on the metal complexes, their unique characteristics and possible applications. Chemical industry requires these days the endless development of chiral catalyst, photoactive compounds, or mild CH and CC bond activating agents just to mention the hottest topics. In pharmaceutical industry green chemistry is the standard. In order to copy metalloenzymes and to find a better way to mimic their reactions there is a continuous challenge for science to create new, efficient complexes.

3.1. Complexes of 3B to 6B metals

Vanadium, chromium and molybdenum are typical candidates for complex formation from group B elements. Interestingly, only two papers have been reported with BII ligands from the same author Baird *et al*. up to this date.[55,56] Dimolybdenum was chosen to synthesize planar molecules with BPI (**7**) and 4′,6′-Me_2BPI (**35**) ligands. One of the complexes was successfully characterized by X-ray revealing an unusual coordination mode (Fig. 3).

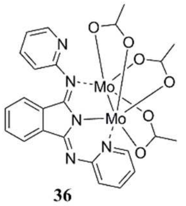

36

Fig. 3. A dimolybdenum complex (**36**) with BPI (**7**)[56]

As a remarkable feature of **36**, one molybdenum ion is coordinated to an imino nitrogen rotating a pyridyl arm into a position where binding to the dimetal unit is not possible. Similar "imino binding" has been documented only once with an aliBII ligand[32] [1,3-bis(isopropylimino)isoindolinate] but it could be expected in that case on the account of missing coordinating sidearms.

3.2. Complexes of 7B metals

Among the biogenic elements manganese has a distinctive role. A large variety of enzymes bear manganese(II or III) cofactor. Most of them participate in the defense mechanism against superoxide free radicals such as superoxide dismutase (SOD)[57] and catalase enzymes.[58] All those BII complexes that have been created contain only this element from group 7B (Table 2).

Table 2
Manganese complexes of BIIs

Ligand	Complex	N_{Py} – Mn (Å)^a	N_{ind} – Mn (Å)^b	τ	Ref.
	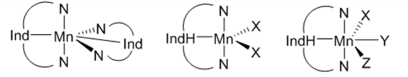 **37, 39, 40, 43, 44, 45, 46** **38, 42** **41**				
7	$[Mn^{II}(ind)_2]$ (**37**)	2.295	2.163, 2.143	-	[49]
7	$[Mn^{II}(indH)Cl_2]$ (**38**)	2.249	2.153	0.69	[17]
11	$[Mn^{II}(3'Me\text{-}BPI)_2]$ (**39**)	2.293	2.144, 2.151	-	[21]
8	$[Mn^{II}(4'Me\text{-}ind)_2]$ (**40**)	-	-	-	[49]
12	$[Mn^{II}(6'Me_2indH)(H_2O)_2(CH_3CN)](ClO_4)_2$ (**41**)	-	-	-	[16]
9	$[Mn^{II}(bimindH)Cl_2](DMF)$ (**42**)	1.959	2.007	0.93	[50]
9	$[Mn^{II}(bimind)_2]$ (**43**)	-	-	-	[15]
13	$[Mn^{II}(Mebimind)_2]$ (**44**)	-	-	-	[15]
10	$[Mn^{II}(BTI)_2]$ (**45**)	2.220	2.211, 2.220	-	[15]
10	$[Mn^{III}(BTI)_2]$ (**46**)	2.146	1.968, 1.967	-	[59]

^{a} The average pyridyl N – Mn distance; ^{b} The isoindoline N(H) – Mn distance

Table 2. contains the characteristic data of the manganese complexes of BIIs. The complexes are identified using the abbreviations reported in the original manuscripts with the corresponding R-group from Figure 2, being denoted for reference with this review. Tau values are valid only for five coordinate structures. The numbers show a nearly perfect trigonal bipyramid (**42**) and an average, moderately distorted TBPY (**38**). The influential factors such as oxidative atmosphere, bases and the right anion that greatly determine the BII structure will be described in the section of Fe-group elements due to the greater amount of research data. The distance between the amino group of the isoindoline core and the metal ion varies in a narrow interval among the manganese complexes. The difference is prominent at +2 (**45**) and +3 (**46**) oxidation states when the same ligand coordinates that can be explained by Jahn-Teller effect. Fig. 4 also emphasizes this difference. Only the Mn^{2+} complexes fit to a linear tendency with the increasing N_{ind} – Mn^{2+} distance.

3.3. Complexes of 8B metals

Iron, cobalt and nickel complexes of BIIs are reported in the greatest number. Compared to manganese, iron also has the affinity to form a broad scale of oxygen adducts. Hereafter, less surprisingly $Fe(R'\text{-}BPI)_x$ (x = 1,2) are likely to be applied and tested as enzyme models.[22,34,62,64,66]
Cobalt and nickel complexes of the title ligands are fairly rare although they have been used multiple times in the oxidation, hydroxylation of hydrocarbons (see also chapter 4.2.).[60,61] The "pincer" shape is also an optimal platform for enantioselective catalytic reactions.[36] Interaction with DNA have been studied in order to develop DNA cleaving therapeutic agents and non-radioactive probes for DNA through Co(BPI)s.[62]

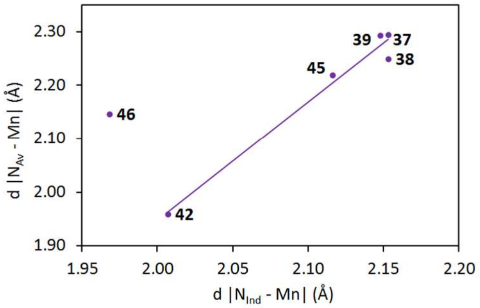

Fig. 4. Bond regularities in the coordination sphere of manganese-BII complexes

3.3.1. Complexes of Fe-group

The most diverse group in this section is undoubtedly the series of complexes created from Fe^{2+} or Fe^{3+}. Iron is not only one of the cheapest metals but also several of its salts are easily accessible. This gives the opportunity to create numerous and versatile new compounds. Considering the great number of iron complexes only the ones with known X-ray structure have been presented in Table 3.

Table 3.
Iron complexes of BIIs

Ligand	Complex	N_{Py} – Fe (Å)[a]	N_{ind} – Fe (Å)[b]	τ (Φ)	Ref.
	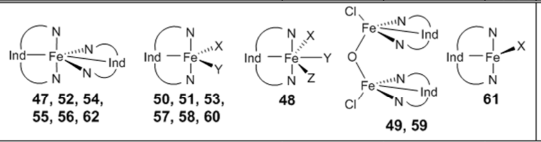 47, 52, 54, 55, 56, 62 50, 51, 53, 57, 58, 60 48 49, 59 61				
7	[Fe^{II}(ind)$_2$ (**47**)	2.240	2.069	-	[48]
7	[Fe^{II}(ind)(CH_3CN)$_3$](ClO_4)$_2$ (**48**)	2.200	2.072	-	[34]
7	[Fe_2^{III}(μ-O)(ind)$_2$$Cl_2$]THF (**49**)	2.153	1.998	0.88	[63]
7	[Fe^{III}(ind)Cl_2 (**50**)	2.148	1.963	0.86	[64]
8	[Fe^{III}(4´Me-ind)Cl_2] (**51**)	2.144	1.978	0.77	[65]
9	[Fe^{III}(bimind)$_2$] (**52**)	1.979	1.912, 1.928	-	[51]
9	[Fe^{II}(bimind)Cl_2] (**53**)	2.067	2.045	-	[66]
13	[Fe^{II}(Mebimind)$_2$] (**54**)	2.136	2.057, 2.053	-	[22]
10	[Fe^{III}(BTI)$_2$] MeCN (**55**)	2.002	1.946, 1.952	-	[22]
10	[Fe^{III}(BTI)$_2$] (**56**)	1.982	1.928, 1.922	-	[59]
10	[Fe^{III}(BTI)Cl_2] (**57**)	2.095	2.019	0.83	[65]
14	[Fe^{III}(5´Me-BTI)Cl_2] (**58**)	2.098	2.029	0.59	[67]
15	[Fe_2^{III}(μ-O)(benzBTI)$_2$$Cl_2$] (**59**)	2.165	2.064, 2.052	0.76	[68]
16	[Fe^{II}Cl(DMSO)(thqbpi)] (**60**)	2.169	1.996	0.31	[69]
16	[Fe^{II}(thqbpi)(CH_2SiMe_3)] (**61**)	2.194	2.002	0.65	[70]
7	[Fe^{II}(4-MeBPI)$_2$] (**62**)	2.085	1.979	-	[61]

[a] The average pyridyl N – Fe distance; [b] The isoindoline N(H) – Fe distance

A large number of transition metal complexes of BIIs have been reported by Robinson *et al*. in 1967.[71] Unfortunately, at this time the lack of accurate analytical techniques limited the clear insight into fine structures. Nowadays, it is known that anions may participate in the inner and outer coordination sphere of the crystals. Similar roles have been assigned to solvent molecules too. The presence of water or non-inert atmosphere increases the chance of oxo-bridged formulations or the replacement of either anions or other solvents in the first coordination sphere (or inner sphere). Based on the available structures and synthetic procedures some conclusions can be made on complex formation. The iron(II)perchlorate and acetate salts tend to result in a 2:1 (ligand-metal) complex (**52**, **54**, **62**, furthermore **37**, **39** with manganese content) mainly with a help of some base (eg. triethylamine). In the absence of any base and under inert atmosphere protonated 1:1 complex can be achieved in a good coordinating solvent such as acetonitrile (**48**). Chlorides seem to favor the *TBPY-5* set. There are only 1:1 complexes reported both with iron(II) and iron(III)chlorides (**50**, **51**, **58**, similarly with Mn: **38**, **42**). Two precedents show that a μ-oxo bridge forms between two iron cores with $FeCl_3$ (**49**, **59**) under air.

In spite of the attempts to obtain $Fe^{II}(BTI)_2$ two independent work proved the viability of $Fe^{III}(BTI)_2$ (**55**, **56**) submitted almost at the same time.[22,59] They are seemingly identical (if anions are ignored) but X-ray structures reveal more. If average $N_{aromatic}$ – Fe distances are plotted against N_{Ind} – Fe distances high- and low-spin complexes can be separated (Fig. 5). There is Mössbauer spectra available to support the high-spin nature of **47** and **54**.[22,48] In a work by Pap *et al*. a low-spin Fe^{3+} complex (**52**) has been synthesized from its high-spin Fe^{2+} counterpart.[51] **55** was obtained from the Fe^{2+} form as well but less harsh conditions were applied.[22] At the same time **56** was prepared directly from a Fe^{3+} salt undoubtedly creating a high-spin complex.

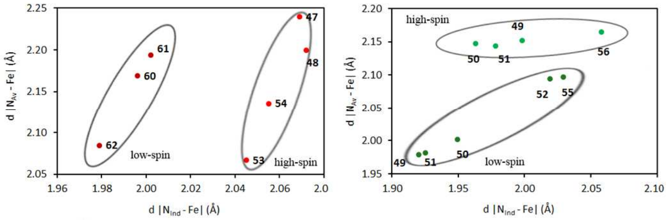

Fig. 5. High and low spin Fe^{2+} (left) and Fe^{3+} (right) complexes

The only ruthenium complexes of BII available in literature have been presented by Pitchumony *et al*.,[72] Gagné *et al*.[73,74] and Tseng *et al*.[75] all together with three X-ray structures (**63-65**) (Fig. 6). Ligands **7**, **8** and **12** (respectively) were involved in the investigations. The resolved structure in the first case (**63**) contains a ligand fracture (1,2-dicyanobenzene) impurity that has an unusual monodentate connection to the metal center. Ruthenium complexes of **8** have been synthesized in various forms, just as Ru(4´-MeLH)Cl_3 and Ru(4´-MeL)$_2$. They were identified by spectroscopic methods and electrochemical and catalytic oxidative properties were tested. Complexes of **12** have PPh_3 coligands Ru^{II}(6´Me-BPI)(PPh_3)Cl (**64**) and HRu^{II}(6´Me-BPI)(PPh_3)$_2$ (**65**). They catalyze base-free and chemoselective alcohol dehydrogenation.

3.3.2. Complexes of Co-group

Asymmetric hydrosilylation, radical polymerization, hydroxylation of hydrocarbons among others have been the chemical aims of the synthesis of CoBIIs. Catalytic efficacy is often compared to salen (salicylaldehyde-ethylenediamine) complexes,[15,34,60] although the N,N,O,O coordination mode strongly differs from BII.

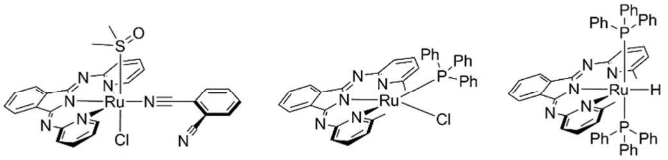

63 **64** **65**

Fig. 6. Representation of known ruthenium structures (**63-65**)[72,75]

Table 4.
Cobalt complexes of BIIs

Ligand	Complex	N_{Py} – Co (Å)[a]	N_{ind} – Co (Å)[b]	τ (Φ)	Ref.
	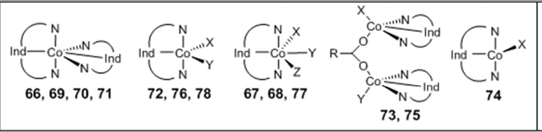 66, 69, 70, 71 72, 76, 78 67, 68, 77 73, 75 74				
7	[Co^{III}(ind)$_2$](ClO$_4$) MeOH (**66**)	1.985	1.889	-	[62]
7	[Co^{III}(BPI)(OBz)(OO-*t*-Bu)] (**67**)	1.955	1.845	-	[60]
9	[Co^{II}(bimind)OAc DMF] (**68**)	2.093	2.040	-	[66]
10	[Co^{II}(BTI)$_2$] (**69**)	2.137	2.069, 2.073	-	[53]
10	[Co^{III}(BTI)$_2$]) (**70**)	1.959	1.913, 1.931	-	[59]
11	[Co^{II}(3´Me-ind)$_2$] (**71**)	2.196	2.004, 2.005	-	[76]
16	[Co^{II}Cl(Me$_2$SO)(thqbpi)] (**72**)	2.161	1.941	0.51	[69]
16	[Co$_2^{II}$(OAc)(thqbpi)$_2$(MeOH)(EtOH)] (**73**)	2.148	1.941, 1.939	0.54	[69]
17	[Co^{II}(CH$_2$SiMe$_3$)(pentbpi)] (**74**)	2.076	1.949	0.67	[37]
18	[Co$_2^{II}$(dihexyl-*t*Bu-bpi)$_2$(OAc)] (**75**)	2.126	1.983, 1.975	0.71	[77]
19	[Co^{II}(acac)(5´chloro-bpi)] (**76**)	2.159	1.969	0.64	[77]
19	[Co^{II}(acac)(3,4-dichloro-5´chloro-bpi)(MeOH)] (**77**)	2.177	2.021	-	[77]
19	[Co^{II}(acac)(3,4-dichloro-5´chloro-bpi)] (**78**)	2.156	1.972	0.50	[77]

[a] The average pyridyl N – Co distance; [b] The isoindoline N(H) – Co distance

Cobalt complexes of any kind favor the octahedral symmetry more than any other metals. The absence of the Werner-type arrangement is observed only in a couple of cases (**72**, **73**, **75**, **76**, **78** - Table 4). **75**-**78** from these molecules have been intentionally converted to the *TBPY-5* structure in order to investigate activity in radical polymerization.[77] A rarely identified structure of **74** was achieved by pyridine displacement from the metal dialkyl precursor (py)$_2$Co(CH$_2$SiMe$_3$)$_2$.

The two other members – rhodium and iridium – of this group belong to the rarest elements of the Earth's crust. A paper by Gade's research group presented a BII complex of the second densest element. Ir^{I}(**18**)(COD) with cyclooctadiene coordination was successfully identified by X-ray resulting in a *OC-6* structure.[78] **18** behaves as a bidentate ligand that was observed only at lanthanides[32] and at aliBIIs. A greater number of carbonyl complexes of the corresponding metals with aroBIIs were reported by Siegl.[79] These compounds were identified by IR and elemental analysis and their reactivity toward alkyl and acyl halides was tested.

3.3.3. Complexes of Ni-group

The very first complexes with the new monoanionic BPI ligands were prepared from Ni by Elvidge & Linstead in the early 1950's.[1] Homoleptic, bidentate Ni(BPI)$_2$ formula was suggested based on UV-Vis and elemental analysis. In the presence of acetate anion it changes to four coordinate 1:1 square-planar complex. It complies with **83** that was synthesized from nickel(II)chloride and **80** that originates from another halogenated Ni complex (Table 5). Further acetato and chloro complexes have been prepared by Siegl[7] from aminopyridine-BPI derivatives. The 2:1 complexes (**79**, **81**) could form with the help of deprotonating triethylamine.

The enantioselective fluorination of oxindoles and β-ketoesters to the corresponding products is effectively catalyzed by **83** with high *ee* and noteworthy yield.[36]

Table 5.
Nickel complexes of BIIs

Ligand	Complex	N_{Py} – Ni (Å)[a]	N_{ind} – Ni (Å)[b]	Φ	Ref.
	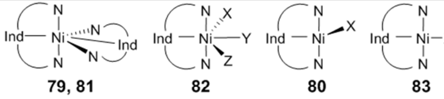 79, 81 82 80 83				
7	[Ni^{II}(ind)$_2$] (**79**)	2.168	2.024	-	[15]
7	[Ni^{II}(ind)(2-Clpcyd)] (**80**)	1.965	1.827	-	[80]
8	[Ni^{II}(4´Me-ind)$_2$] (**81**)	2.180	2.017	-	[15]
9	[Ni^{II}(bimind)OAc DMF] (**82**)	2.069	2.011	-	[66]
20	[Ni^{II}(boxmi)Cl] (**83**)	1.911	1.904	0.07	[36]

[a] The average pyridyl N – Ni distance; [b] The isoindoline N(H) – Ni distance

The most redundant group of isoindoline complexes is undoubtedly the one with palladium core. Its popularity can be attributed to the cyclopalladation phenomena. Unlike with other transition metals, unique N,N,C type coordination can occur with BII that was documented by Dietrich *et al.*[39] Steric hindrance on the pyridyl moiety and palladium excess are the influential factors of cyclometallation.[40] The flexibility of BIIs allows a flip on the axis of one C-N bond that is attributed to an intramolecular strain.[41] After C-H and C-C bond activation takes place further Pd^{II} can coordinate to exocyclic N atoms (**87**). Exploiting this remarkable feature of palladium S-coordination (**114**) was observed on one thiazole subunit of BTI ligand (**26**) that was unprecedented before (Fig. 7).[86]

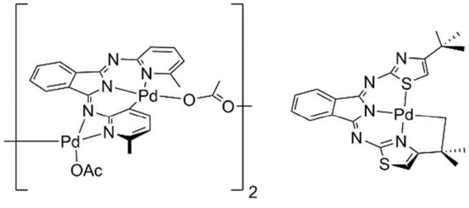

87 **114**

Fig. 7. Exocyclic- (left) and S-coordination (right) of palladium complexes[41,86]

All Pd complexes are planar or pseudoplanar, no other structures have been recorded. Unsymmetrical complexes were not included in Table 6. Kleeberg and Bröring reported a series of such complexes with unusual structural features.[43] The new complexes had *t*Bu-selenazol-pyridine and *t*Bu-thiazole-pyridine sidearms on their ligands. In both of their packing pattern large voids were comprised that could be suitable even for small molecule storage according to the authors.

The small number of platinum complexes (Table 7) have similar structural motives to the ones in the previous chapter. Most of them was presented by Wen *et al.*[19,87] They have square-planar geometry around the metal ion with chloride and aromatic coligands. Photophysical properties like luminescence are in the focus of recent research in both biologic (ion sensors) and industrial solutions (photocatalytic hydrogen production).

Fig. 8 shows a good correlation between tetrahedricity factor (Φ) and endocyclic amine-palladium distances. The increasing central N$_{ind}$-Pd distance is in agreement with the degree of distortion that is nearly negligible in **107** and the highest in **103**. The unique structure of **115** and the N,N,S coordination of **114** likely explain their deviation from the well-observed trend.

The small structural differences of platinum complexes resulted in similar Φ values with 5 % deviation (Fig. 8 inset). Distorting factors have a minimal influence on the structures so the trend can be considered zero. This indicates that neither anions nor ligands-coligands can influence the electronic structure of Pt^{2+}.

Table 6.
Palladium complexes of BIIs

Ligand	Complex	N_{Py} – Pd (Å)[a]	N_{ind} – Pd (Å)[b]	Φ	Ref.
	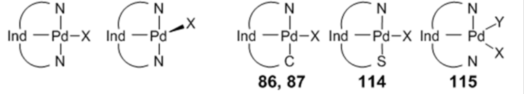 **86, 87** **114** **115**				
7	$[Pd^{II}(BPI)(OAc)]$ (**84**)	2.038	1.946	0.13	[41]
8	$[Pd^{II}Cl(4\text{-}(HOCH_2CH_2)\text{-}10\text{-}MeBPI)]$ (**85**)	2.063	1.965	0.09	[81]
12	$[Pd^{II}(6'Me\text{-}ind)(Cl)]$ THF (**86**)	2.152	1.967	0.19	[39]
12	$[Pd^{II}_4(6'Me\text{-}BPI)_2(OAc)_4]$ (**87**)	2.174	1.987	0.16	[41]
18	$[Pd^{II}Cl(4\text{-}Me\text{-}10\text{-}t\text{BuBPI})]$ (**88**)	2.065	1.957	0.18	[18]
21	$[Pd^{II}Cl(11\text{-}Me\text{-}BPI)]$ (**89**)	2.058	1.93, 1.94	0.09	[18]
22	$[Pd^{II}Cl(11\text{-}Br\text{-}BPI)]$ (**90**)	2.061	1.962	0.16	[18]
23	$[Pd^{II}Cl(11\text{-}TMS\text{-}ethynyl\text{-}BPI)]$ (**91**)	2.049	1.958	0.21	[18]
24	$[Pd^{II}Cl(11\text{-}Ph_3Si\text{-}ethynyl\text{-}BPI)]$ (**92**)	2.031	1.952	0.23	[18]
25	$[Pd^{II}(pinBPI)(OAc)]$ (**93**)	2.053	1.936	0.04	[38]
25	$[Pd^{II}Cl(pinBPI)]$ (**94**)	2.053	1.962	0.20	[38]
26	$[Pd^{II}(4\text{-}MeBTI)(OC(NH_2)Me)]^+ BAr^{F-}$ (**95**)	2.036	1.968	0.29	[82]
26	$[Pd^{II}(4\text{-}MeBTI)(dmf)]^+ BAr^{F-}$ (**96**)	2.026	1.968	0.24	[82]
26	$[Pd^{II}(4\text{-}MeBTI)(OCHO)]^+ BAr^{F-}$ (**97**)	2.034	1.976	0.17	[82]
26	$[Pd^{II}(4\text{-}MeBTI)(OC(NHPh)_2)]^+ BAr^{F-}$ (**98**)	2.045	1.962	0.19	[82]
26	$[Pd^{II}(4\text{-}MeBTI)(SMe_2)]^+ BAr^{F-}$ (**99**)	2.024	2.009	0.36	[82]
26	$[Pd^{II}(4\text{-}MeBTI)(SeMe_2)]^+ BAr^{F-}$ (**100**)	2.020	2.010	0.36	[82]
26	$[Pd^{II}(4\text{-}MeBTI)(OAc)]$ (**101**)	2.046	1.978	0.21	[83]
26	$[Pd^{II}(4\text{-}MeBTI)(Cl)]$ (**102**)	2.038	1.998	0.33	[83]
26	$[Pd^{II}(4\text{-}MeBTI)(PMe_3)]\ B(Ar^F)_4$ (**103**)	2.018	2.036	0.44	[84]
26	$[Pd^{II}(4\text{-}MeBTI)(t\text{BuNH}_2)]\ B(Ar^F)_4$ (**104**)	2.030	1.988	0.34	[84]
26	$[Pd^{II}(4\text{-}MeBTI)(PhNH_2)]\ B(Ar^F)_4$ (**105**)	2.031	1.974	0.28	[84]
26	$[Pd^{II}(4\text{-}MeBTI)(Py)]\ B(Ar^F)_4$ (**106**)	2.064	1.973	0.03	[84]
26	$[Pd^{II}(4\text{-}MeBTI)(2,6\text{-}Me_2py)]\ B(Ar^F)_4$ (**107**)	2.055	1.969	0.01	[84]
26	$[Pd^{II}(4\text{-}MeBTI)(MeCN)]\ B(Ar^F)_4$ (**108**)	2.044	1.961	0.28	[84]
26	$[Pd^{II}(4\text{-}MeBTI)(MeNC)]\ B(Ar^F)_4$ (**109**)	2.048	2.000	0.27	[84]
27	$[Pd^{II}(3,6\text{-}MepMeOi)(OAc)]$ (**110**)	2.078	1.957	0.27	[85]
27	$[Pd^{II}(3,6\text{-}Me_2\text{-}BPI)(OAc)]$ (**111**)	2.082	1.949	0.27	[41]
28	$[Pd^{II}(iPrBTI)(OAc)]$ (**112**)	2.027	1.989	0.21	[85]
29	$[Pd^{II}(6\text{-}Me\text{-}bpmi)(OAc)]$ (**113**)	2.054	1.958	0.02	[41]
30	$[Pd^{II}(4\text{-}t\text{Bu-BTI})]$ (**114**)	1.986	2.076	0.03	[86]
30	$[Pd^{II}(4\text{-}t\text{Bu-BTI})(Py)]$ (**115**)	2.010	2.132	0.09	[86]

[a] The average pyridyl N – Pd distance; [b] The isoindoline N(H) – Pd distance

Table 7.
Platinum complexes of BIIs

Ligand	Complex	N_{Py} – Pt (Å)[a]	N_{ind} – Pt (Å)[b]	Φ	Ref.
	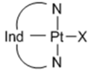				
7	$[Pt^{II}(BPI)(pyridine)(PF_6)]$ (**116**)	2.058	1.964	0.15	[87]
7	$[Pt^{II}(BPI)(C{\equiv}CC_6H_5)]$ (**117**)	2.046	1.985	0.10	[19]
7	$[Pt^{II}(BPI)(C{\equiv}CC_6H_4Bu^t\text{-}4)]$ (**118**)	2.050	1.995	0.13	[19]
7	$[Pt^{II}(HL_3BPI)(Cl)]$ (**119**)	2.039	1.977	0.11	[19]
18	$[Pt^{II}Cl(4\text{-}Me\text{-}10\text{-}t\text{BuBPI})]$ (**120**)	2.055	1.966	0.12	[81]

[a] The average pyridyl N – Pt distance; [b] The isoindoline N(H) – Pt distance

Fig. 9 shows how tetrahedricity factor (Φ) has been calculated in case of palladium complexes from the opposite planes of a molecule. The method was described on Scheme 3 however the diversity of Pd complexes allows an expressive representation. The angle between planes 1-2 (ϕ_1) and planes 3-4 (ϕ_2) is small as expected for square planar complexes and increases as distortion grows towards the tetrahedral form. The largest angle (ϕ_0) is close to 90° for both *SP-4* and *T-4* in an ideal case.

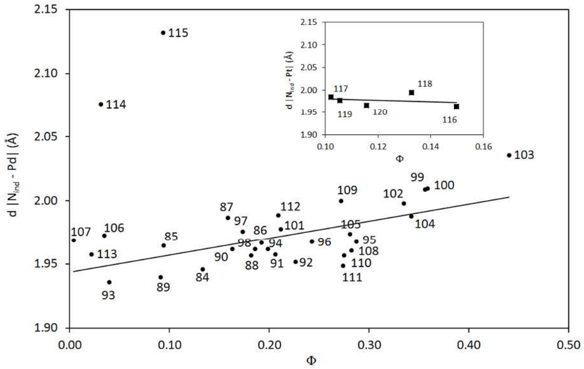

Fig. 8. Correlation between tetrahedricity factor and metal-indoline distances

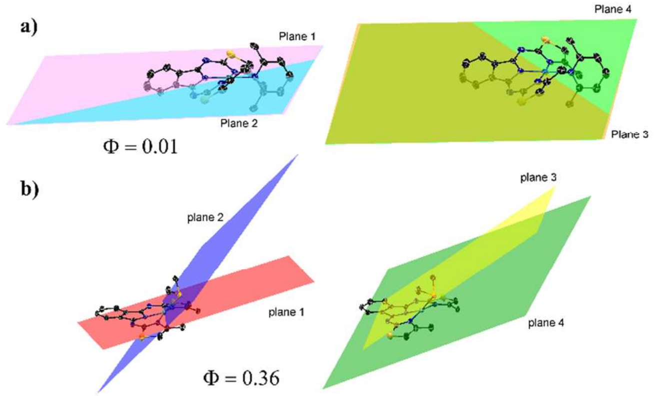

Fig. 9. Representative planes in four-coordinate complexes **107** (a) and **100** (b) for the calculation of tetrahedricity factor (Φ)

3.4. Complexes of 1B metals

From the group of 1B elements only copper containing molecules have been synthesized with BIIs (Table 8). Octahedral, trigonal-bipyramidal, furthermore the transition between tetrahedral and square-planar geometries appear in various structures. Similarly to manganese a large number of enzymes contain copper as co-factor. Model complexes of SOD, quercetinase or catechol oxidase are known to have considerable mimicking activities.

$Cu(3'MePyOIND)_2$ (**142**) (Fig. 10.) belongs to the unsyBII family with a tetrahedral arrangement of ligands around the copper center.[23] The complex was found to exhibit catecholase activity by catalyzing the conversion of 3,5-di-*tert*-butylcatechol to 3,5-di-*tert*-butylbenzoquinone. Same activity and similar catalytic strength was found for **126** however their coordination sphere is different. Certainly, an incomplete third arm on BII gives the advantage of tunable (hydrophilicity, hydrophobicity, chirality, *etc.*) 2:1 complexes while enough space remains for substrate accessibility. Other unsymmetric bidentate isoindoline compounds have been reported to possess antiproliferative activity (**143**, **144**).[10]

Stability and redox inactivity have been proved of *OC-6* 2:1 complexes (**132**, **133** and derivatives with ligands: **7**, **8**, **9**, **13**, **15**). Their 1:1 counterparts (**121**, **134**, **135** and derivatives with the same ligands) effectively participated in superoxide scavenging reactions mimicking SOD enzymes.[46]

Table 8.
Copper complexes of BIIs

Ligand	Complex	N$_{Py}$ – Cu (Å)^a	N$_{ind}$ – Cu (Å)^b	τ (Φ)	Ref.
	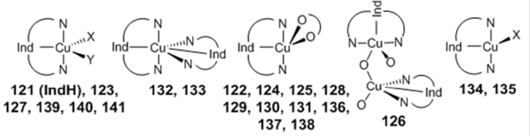 121 (IndH), 123, 127, 139, 140, 141 · 132, 133 · 122, 124, 125, 128, 129, 130, 131, 136, 137, 138 · 126 · 134, 135				
7	[Cu^{II}(BPIH)(NCCH$_3$)(OClO$_3$)] (**121**)	2.020	1.911	0.21	[46]
7	[Cu^{II}(4-MeBPI)(OAc)] (**122**)	2.019	1.884	-	[88]
7	[Cu^{II}(ind)(pga)(H$_2$O)] (**123**)	2.027	1.902	0.21	[47]
7	[Cu^{II}(ind)(mco)] (**124**)	2.041	1.905	0.38	[89]
7	[Cu^{II}(NBAII)(OAc)] (**125**)	2.003	1.895	-	[90]
8	[Cu$_2^{II}$(4´Me-ind)$_2$(MeOH)(μ-OH)]ClO$_4$ MeOH (**126**)	2.017	1.920, 1.906	0.36	[91]
8	[Cu^{II}(4´Me-ind)(H$_2$O)$_2$]ClO$_4$ (**127**)	1.979	1.904	0.66	[92]
9	[Cu^{II}(bimind)(pga)] 2 DMF (**128**)	1.947	1.934	-	[47]
9	[Cu^{II}(bimind)(ba)] DMF (**129**)	1.950	1.931	-	[47]
9	[Cu^{II}(bimind)OAc] (**130**)	1.967	1.949	-	[66]
10	[Cu^{II}(BTI)(OAc)] (**131**)	1.968	1.960	-	[88]
10	[Cu^{II}(BTI)$_2$] (**132**)	2.181	2.001, 1.983	-	[46]
11	[Cu^{II}(3´Me-ind)$_2$] (**133**)	2.265	1.952, 1.948	-	[46]
13	[Cu^{II}(Mebimind)(Cl)] 0.5 CH$_2$Cl$_2$(**134**)	1.956	1.945	0.44	[46]
15	[Cu^{II}(benzBTI)(Cl)] C$_7$H$_8$ (**135**)	1.987	1.928	0.48	[46]
31	[Cu^{II}(tetraphenyl-pinBPI)(OAc)] (**136**)	2.094	1.883	-	[13]
32	[Cu^{II}(Me-pentBPI)(OAc)] (**137**)	2.038	1.912, 1.905	-	[93]
33	[Cu^{II}(Bn-pentBPI)(OAc)] (**138**)	2.050	1.898	-	[93]
32	[Cu^{II}(OMe-pentBPI)(Cl)] (**139**)	2.029	1.913	0.36	[93]
33	[Cu^{II}(Bn-pentBPIH)(CF$_3$SO$_3$)$_2$] (**140**)	1.941	1.902	0.52	[93]
33	[Cu^{II}(Bn-pentBPI)(CF$_3$SO$_3$)] H$_2$O (**141**)	1.932	1.887	0.58	[93]

[a] The average pyridyl N – Cu distance; [b] The isoindoline N(H) – Cu distance

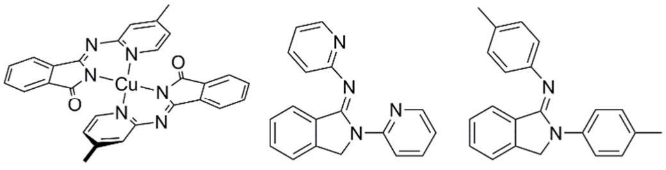

142 **143** **144**

Fig. 10. UnsyBII ligands and a complex with copper[10,23]

3.5. Complexes of 2B metals

Metals of group 2B or group 12 are considered highly toxic except zinc that is contrarily among the most important metals in public health. Enzymes with zinc active center are widespread in living organisms therefore deficiency may lead to growth retardation while excess of it unsettles the sensitive biogenic metal balance.

The stable d^{10} electron configuration of Zn^{2+} has a strong impact on complex formation with BIIs. Conventional methods like using triethylamine base in order to deprotonate the ligand are usually insufficient.[69,92,94] The two structures of **147** and **148** (Table 9) have been obtained with tetra-*n*-butylammonium hydroxide, although some parts in **148** may have remained nondeprotonated.[94] **151** and **152** have been synthesized *in situ* from the ligand precursor using the metal salt as catalyst.

Table 9.
Zinc complexes of BIIs

Ligand	Complex	N$_{Py}$ – Zn (Å)^a	N$_{ind}$ – Zn (Å)^a	τ	Ref.
	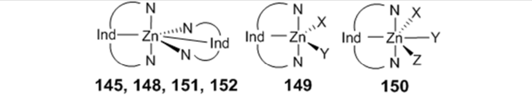 145, 148, 151, 152 · 149 · 150				
7	[Zn^{II}(ind)$_2$] (**145**)	-	-	-	[21]
7	[Zn^{II}(NBAII)(OAc)] (**146**)	-	-	-	[90]
8	[Zn$^{II}_3$(4´Me-ind)$_4$] (ClO$_4$)$_2$ 5 H$_2$O (**147**)	2.020	1.930	-	[92]
8	[Zn^{II}(4´Me-ind)$_2$] (**148**)	2.243	2.053, 2.038	-	[94]
9	[Zn^{II}(bimind)OAc DMF] (**149**)	2.083	2.064	-	[66]
10	[Zn^{II}(BTI)(OMe)$_3$] (**150**)	2.094	2.056	-	[59]
20	[Zn^{II}(Phbox)$_2$] (**151**)	2.168	2.121	-	[95]
34	[Zn^{II}(*i*Prbox)$_2$] (**152**)	2.170	2.174	-	[95]

[a] The average pyridyl N – Zn distance; [b] The isoindoline N(H) – Zn distance

Table 10.
Cadmium complexes of BIIs

Ligand	Complex	N$_{Py}$ – Cd (Å)^a	N$_{ind}$ – Cd (Å)^b	τ	Ref.
	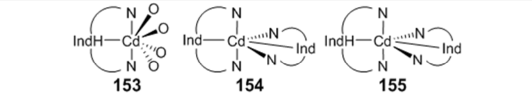 153 · 154 · 155				
8	[Cd^{II}(4´Me-indH)(NO$_3$)$_2$] MeOH (**153**)	2.303	2.234	-	[97]
8	[Cd^{II}(4´Me-ind)$_2$] (**154**)	2.374	2.258, 2.233	-	[94]
8	[Cd^{II}(4´Me-ind)(4´Me-indH)] ClO$_4$ (**155**)	2.363	2.264, 2.251	-	[94]

[a] The average pyridyl N – Cd distance; [b] The isoindoline N(H) – Cd distance

The lack of complete deprotonation occurred in **155** (Table 10). The flexibility of the isoindoline system allows the shuttling of the iminium proton between imine N atoms. This intramolecular proton transfer was followed by ^{1}H NMR spectroscopy.[94,97] The three Cd structures (**153**- **155**) with their preparative circumstances perfectly represent the coordinative capacities of monoanionic aroBIIs.

The last paper to be overviewed is an individual work on a mercury compound by Wicholas' group. The coordination pattern of Hg resembles **153** that is not surprising because similar reaction conditions have been applied. The outer sphere solvent and the inner sphere anion coligand are the dissimilarities [Hg$^{II}_3$(4´Me-ind)$_4$] (NO$_3$)$_2$ 4 MeOH.[96]

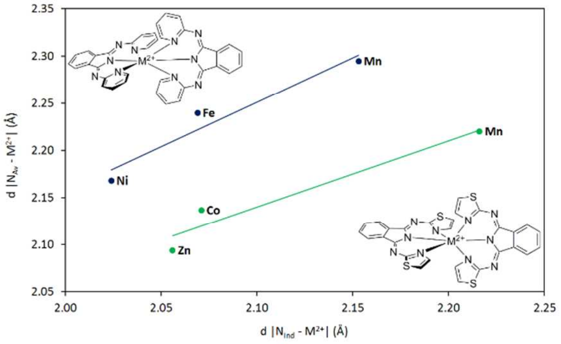

Fig. 11. The Irving-Williams type stability of transitional metal complexes with **7** and **10**

As a closure of this section regularities in complex stability have been drafted with complex series of the same ligands. The stability of isoindoline complexes is rarely determined by the *K* constant. Fortunately, a stability order was found by Irving and Williams for high-spin complexes of divalent metal ions in the middle of the previous century.[98] The combination of knowledge in Jahn-Teller effect, Crystal Field Stabilization Energy and ionic radius is the key to explain the series. Since it stands for a wide variety of ligands, it was found to be suitable for ligands **7** and **10** as well (Fig. 11). Bond distances of isoindoline N_{ind}-M^{2+} and N_{Py}-M^{2+} show the same pattern with the Irving-Williams series.

3.6. Complexes of aminophthalazines (PAP)

Metal chelating capacity and the simplicity of synthesis makes PAPs excellent "isoindoline-based" ligands. The most eye-catching difference from isoindolines is the vicinal N atoms that determine the structural arrangement of metals creating a perfect environment for bi-, or trinuclear complexes. The bidentate coordination and the proximity of metal ions forms oxo-, halogenato or even azido-bridges in several occasions. Thompson *et al*. presented the first synthesis of PAP[14] in 1969 and focused on nickel, copper and cobalt complexes later on in his work (Table 11).[102-105] The only manganese complex has been characterized by spectroscopic methods and elemental analysis suggesting the $[Mn^{II}_2(6'Me_2PAP)_2Cl_2]$ formula.[99]

Table 11.
PAP complexes of transition metals

Ligand	Complex	M – M (Å)	N_{ind} – M (Å)	Ref.
7	$[Cu^{II}_2(PAP)Cl_3(OH)]\ 1.5\ H_2O$ (**156**)	-	2.000-2.038	[14, 100]
7	$[Fe^{II}_2(\mu\text{-}OMe)_2(PAP)Cl_4]\ 2MeOH$ (**157**)	3.021	2.204	[101]
7	$[Co^{II}_2(PAP)_3(OH)_2]\ Br_4\ 9H_2O$ (**158**)	2.795	1.880	[102]
7	$[Ni^{II}_2(PAP)_3(H_2O)_2]\ Br_4\ 6H_2O$ (**159**)	3.390	2.075, 2.084	[102]
35	$[Cu^{II}_2(PAP\text{-}4,6Me)_4Cl_4]$ (**160**)	3.251	2.022,	[103]
7	$[Cu^{II}_4(PAP)_2(\mu_2\text{-}1,1\text{-}N_3)_2(\mu_2\text{-}1,3\text{-}N_3)_2(\mu_2\text{-}CH_3OH)_2(N_3)_4]$ (**161**)	3.207	2.021	[104]
11	$[Cu^{II}_4(PAP\text{-}3Me)_2(\mu_2\text{-}1,1\text{-}N_3)_2(\mu_2\text{-}1,3\text{-}N_3)_2(H_2O)_2(NO_3)_2]\ (NO_3)_2$ (**162**)	3.163	2.009, 1.970	[104]
7	$[Ni^{II}(PAPH)_2(H_2O)_2]\ (BF_4)_4$ (**163**)	-	2.064	[105]
7	$[Ni^{II}_2(PAP)_3(H_2O)_2]\ (NO_3)_4\ 5H_2O$ (**164**)	3.126	2.070, 2.059	[105]
7	$[Co^{III}_2(PAP)_3(OH)_2]\ (NO_3)_4\ xH_2O$ (**165**)	2.777	1.89, 1.91	[105]
7	$[Ni^{II}_3(PAP)_3(OH)_2]\ (BF_4)_3F\ xH_2O$ (**166**)	2.997-3.026	2.048-2.057	[105]
13	$[Fe^{III}_3(MebimPAP)_3O]^+$ (**167**)	3.305-3.33	2.047-2.066	[106]
14	$[Fe^{III}_2(\mu\text{-}OMe)_2(5MeBTI\text{-}PAPH_2)Cl_4]$ (**168**)	3.012	2.249	[68]

4. Applications, aims of development

In approximately 50-60 % of the scientific papers in this subject new molecules are presented only with the purpose of structural characterization. Fundamentally, one has to know about the N,N,N donor title ligands that they are promising carriers of all transition metals leaving their redox properties almost intact. Their tunability is not only a basic requirement but based on the number of publications and the wide variety of new applications found it is reality as well. An aging review on pincer-type complexes[107] pointed the focus on light-harvesting, sensoring and biological approaches in its closing remarks. These remarks are still valid. The increasing need for energy, the development of modern devices and the improvement of human healthcare still fully cover those suggestions in our modern life.

With some perspicuous intention the current major research directions will be discussed in two broader categories such as biomimetics and chemical catalysis.

4.1. Biomimetic studies

Oxidoreductases is a fairly populous subgroup of enzymes that can perform electron or hydrogen atom transfer reactions between the interacting molecules. Some of them with metal content (metalloenzymes) are phenoxazinone synthase (EC 1.10.3.4), catalase (EC 1.11.1.6), catechol oxidase (EC 1.10.3.1), catechol dioxygenase (EC 1.13.11.1-3), methane monooxygenase (EC 1.14.13.25) and superoxide dismutases (EC 1.15.1.1). These representatives are the subjects of continuous research on enzyme mimics related to isoindoline-based bioactive complexes.

4.1.1. Phenoxazinone synthase mimics

Phenoxazinone synthase (PHS) is a member of multicopper-oxydases.[108,109] It catalyzes the oxidative coupling of substituted *o*-aminophenols to produce phenoxazinones that are effective antineoplastic, antitumor agents known as *actinomycin D* and *questiomycin A*.[110,111] PHS mimics is tested with functional models that must have the ability to catalyze the oxidative coupling of *o*-aminophenol (OAPH) to 2-amino-3*H*-fenoxazin-3-on (APX). The reaction progress can be monitored by UV-Vis spectroscopy following the product formation at λ = 435 nm (log ε = 4.20). The general goal of enzyme mimics is not the development towards perfect therapeutics but to have better insight into the actual mechanism. Although, copper is the active metal in PHS, models have been created with cobalt,[112] iron[113] and manganese[114] complexes. The corresponding isoindoline-based compounds have been collected in Table 12. Their catalytic efficacy (k_{cat}/K_M) complies with the other models found in the literature of this topic, furthermore straight correlation was observed between oxidation potential of the iron center in the precursor complex and catalytic efficacy.

Table 12.
Isoindoline-based PHS models and kinetic data

Ligand	Complex	$E°'_{pa}$	k_{cat}/K_M ($M^{-1}s^{-1}$)	Ref.
7	$[Fe^{III}(ind)Cl_2$ (**50**)	415	20.94	[67]
8	$[Fe^{III}(4'Me\text{-}ind)Cl_2]$ (**51**)	251	13.44	[67]
10	$[Fe^{III}(BTI)Cl_2]$ (**57**)	302	10.05	[67]
14	$[Fe^{III}(5'Me\text{-}BTI)Cl_2]$ (**58**)	260	9.93	[67]
15	$[Fe^{III}(benzBTI)Cl_2]$ (**169**)	514	69.25	[67]
12	$[Mn^{III}(6'Me\text{-}indH)(H_2O)_2(MeCN)](ClO_4)_2$ (**170**)	-	0.16	[16]

Two possible mechanisms have been proposed as overall conclusion of PHS mimics with isoindoline complexes. One of them is a metal-based oxidation shown as route 1 in Scheme 4. The rate determining step is the ternary complex formation of metal, ligand and dioxygen that is facilitated by the dioxygen-metal interaction. In the second route a radical formation from H_2O_2 is assumed initiated by the complexes but substrate transformation happens via standard radical pathway. The first available model experiments were carried out by Prati *et al.*[109] and Barry *et al.*[110] around the 1990's. The recent knowledge is still based on the original 3 × 2 e^- oxidation process however, it has been extended to other metals and with some radical involvement.

Recently, as a major improvement an expressive correlation was discovered (Fig. 12) how fine-tuning of the precursor complex could increase reaction rates during AXP synthesis. Modifications on BII strongly influence the oxidation potential of iron complexes that has a straight effect on the reaction rates.

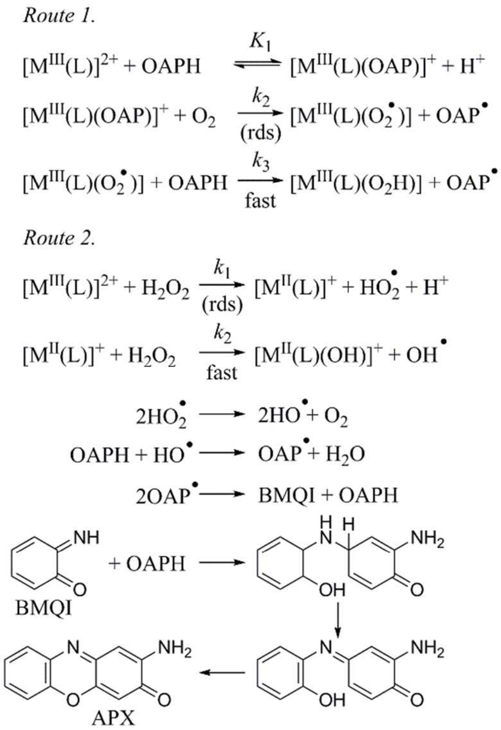

Scheme 4. The proposed mechanism of phenoxazinone synthase model reactions[67]

According to kinetic data a ternary complex formation is plausible among superoxoiron(III), the corresponding ligand and dioxygen (route 1, step 2 in Scheme 4) in the rate determining step.[67]

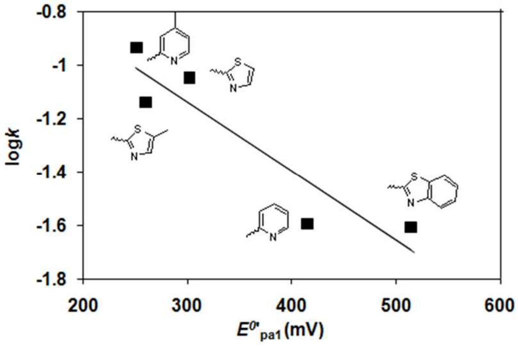

Fig. 12. Isoindoline dependent oxidation potentials in iron complexes vs. reaction rates in phenoxazinone synthase mimics[67]

4.1.2. Catalase mimics

Biological processes at every level of life produce side products. One harmful compound is H_2O_2 that has to be removed from the cellular environment. As a part of the natural defense mechanism of living organisms catalase enzymes (with Mn and Fe centered active sites) are able to facilitate the biodegradation of peroxides. Human catalase is a tetramer polypeptide with heme-type active center in each subunit. Together with some additional amino acids (Tyr358, His75, Asn148) in the direct environment of the Fe^{3+} core the dismutation of H_2O_2 happens into water and dioxygen.[115] Free or "improperly" bonded Fe^{2+} ions tend to generate •OH radicals in a Haber-Weiss reaction (Scheme 5.). As a result similarly noxious reactive oxygen species (ROS) appear that are responsible for organ failures, heart attack or neurodegenerative diseases.[116]

$$Fe^{2+} + H_2O_2 \longrightarrow Fe^{3+} + OH^{\ominus} + \bullet OH$$

Scheme 5. The Haber-Weiss reaction

The catalase activity of manganese complexes has been determined by gas-volumetric method measuring dioxygen evolution from H_2O_2 in specific time intervals. Results are shown in Table 13 compared to the original enzyme efficiency from various sources. The k_{cat}/K_M values of models are significantly lower than catalase, but they are in the same range with other model compounds.[117] The most active compound up to this date is a Mn^{4+} complex with a SALPN type ligand that is still far behind the native enzyme.[118] The hypothetical cycle of mechanism is explained by Mn^{3+} – Mn^{4+} (mononuclear) or Mn^{2+}/Mn^{2+} – Mn^{3+}/Mn^{3+} (dinuclear) transitions.[118,119]

Table 13.
Isoindoline models of catalase

Ligand	Complex	k_{cat}/K_M ($M^{-1}s^{-1}$)	Ref.
-	*T. thermophilus catalase*	3.1×10^6	[117]
-	*L. plantarum catalase*	0.6×10^6	[117]
-	*T. album catalase*	1.7×10^6	[117]
7	$[Mn^{II}(ind)_2]$ (**37**)	3.20	[49]
7	$[Mn^{II}(indH)Cl_2]$ (**38**)	79.2	[17]
8	$[Mn^{II}(4'Me\text{-}ind)_2]$ (**40**)	3.20	[49]
9	$[Mn^{II}(bimindH)Cl_2](DMF)$ (**42**)	4.12	[50]

Considering future directions of developments some useful observations have been made how coligands and other structural changes are able to influence activity. Inactive 1:1 or slightly active 1:2 (metal – ligand ratio) manganese complexes could be enhanced by active molecules such as TEMPO (2,2,6,6-tetramethyl-piperidin-1-yl-oxyl)[120] or different N-donor heterocycles (pyridine, imidazole)[17] (L). Electron-donating moieties on both coligands (changing imidazole to 1-methylimidazole)[17] and R-groups of **3** (more effective **9** than **7**)[50] have increasing effect on activity. On the basis of reaction kinetic data a mechanism has been proposed where Mn(II) is transformed into a Mn(IV)=O species that is reduced by H_2O_2 to its initial form at the end of the catalytic cycle (Scheme 6.)[17]

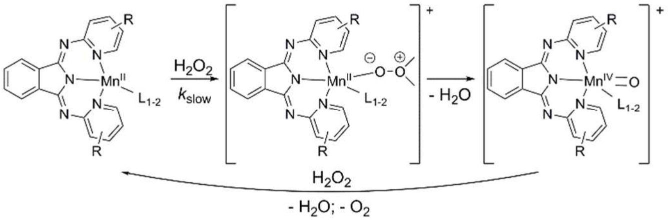

Scheme 6. The proposed mechanism of catalase model reactions[17]

4.1.3. SOD (superoxide dismutase) mimics

Superoxide dismutases have a major role in the destruction of peroxides, superoxides and radical anions in a close relationship with the previously described catalase. They are a group of versatile enzymes that have high metal specificity mostly with Fe and Mn cofactor,[121,122] but certain life forms operate with Cu/Zn-[123] or NiSODs.[124]
McCord–Fridovich assay[125] is a well-known spectrophotometric protocol that is used to determine superoxide dismutase activity. All complexes presented in Table 14 have been tested in a reaction of nitroblue tetrazolium

(NBT) or cytochrome c reduction. The superoxide radical anion ($O_2^{\bullet-}$) was generated in situ by the xanthine/xanthine oxidase reaction, and its decomposition was monitored spectrophotometrically by following the formation of diformazan from NBT at 560 nm, or alternatively, by monitoring the reduction of cytochrome c at 550 nm. The products of the disproportionation are dioxygen and hydrogen peroxide.

Table 14.
Isoindoline models of SOD

Ligand	Complex	E_{pc}[a] ($E_{ox/red}$)	IC_{50} (10^{-6} M)	k_{McF} (k_{cat}) ($10^{-6}M^{-1}s^{-1}$)	Ref.
-	*CuZnSOD*	-	-	2000	[126]
9	$[Cu^{II}(bimindH)(NCCH_3)(OClO_3)]ClO_4$ (**171**)	-0.835	6.62	1.98	[46]
9	$[Cu^{II}(bimindH)Cl_2]$ (**172**)	-0.835	10.99	1.19	[46]
13	$[Cu^{II}(Mebimind)Cl]$ 0.5 CH_2Cl_2 (**134**)	-0.860	27.37	0.48	[46]
10	$[Cu^{II}(BTIH)(NCCH_3)(OClO_3)]ClO_4$ (**173**)	-0.826	4.69	2.80	[46]
10	$[Cu^{II}(BTI)Cl]$ (**174**)	-0.826	7.19	1.83	[46]
7	$[Cu^{II}(BPIH)(NCCH_3)(OClO_3)]ClO_4$ (**121**)	-0.724	0.95	13.82	[46]
7	$[Cu^{II}(indH)Cl_2]$ (**175**)	-0.724	2.06	6.37	[46]
15	$[Cu^{II}(benzBTI)Cl]$ (**135**)	-0.650	1.21	10.85	[46]
10	$[Fe^{II}(BTI)_2]$ (**176**)	(0.555)	-	(5.00)	[22]
10	$[Fe^{II-III}(BTI)_2]$ MeCN (**55**)	-	-	(5.28)	[22]
7	$[Fe^{II}(ind)_2$ (**47**)	(0.319)	-	(3.83)	[22]
8	$[Fe^{II}(4'Me\text{-}ind)_2$ (**177**)	(0.265)	-	(3.62)	[22]
9	$[Fe^{II}(bimind)_2$ (**52**)	(0.205)	-	(3.06)	[22]
13	$[Fe^{II}(Mebimind)_2$ (**178**)	(0.123)	-	(2.50)	[22]
9	$[Mn^{II}(bimind)_2]$ (**179**)	(-0.021)	3.10	(3.28)	[15]
13	$[Mn^{II}(Mebimind)_2]$ (**180**)	(0.005)	6.36	(1.60)	[15]
10	$[Mn^{II}(BTI)_2]$ (**45**)	(0.082)	12.10	(0.83)	[15]
7	$[Mn^{II}(ind)_2]$ (**181**)	(0.015)	8.74	(1.26)	[15]
11	$[Mn^{II}(3'Me\text{-}ind)_2]$ (**182**)	(-0.098)	11.10	(0.99)	[15]
8	$[Mn^{II}(4'Me\text{-}ind)_2]$ (**183**)	(-0.082)	9.44	(1.08)	[15]
7	$[Co^{II}(ind)_2]$ (**184**)	-0.483	4.29	2.35	[53]
11	$[Co^{II}(3'Me\text{-}ind)_2]$ (**185**)	-0.512	4.82	2.10	[53]
8	$[Co^{II}(4'Me\text{-}ind)_2]$ (**186**)	-0.583	15.90	0.64	[53]

[a] Redox potential values are expressed in Volt.

SOD models are categorized by inhibition constant IC_{50} values (nM – μM range, the concentration where inhibition of NBT or cyt c reduction is 50%). Unlike with other enzyme models the primary aim here is the invention of an effective SOD substitute. Kinetic measurements focus on the achievement of lower IC_{50} or higher k_{McF} instead of the understanding of the mechanism. Rather new findings with cobalamins may point to the right direction namely their efficacy approach SOD.[127]
Overviewing the results of SOD mimicking activity it is clear that the transition metal complexes of BIIs are relevant artificial models of SOD function. Redox potentials, coordination geometry and ligands have the key roles in the process. Octahedral complexes with irreversible redox behavior have a little contribution to superoxide destruction.[46,53] Scenic correlation was found between reduction peak potential (E_{pc}) and inhibition constant at copper complexes.[46] Iron activities correlate better with redox potentials ($E_{ox/red}$)[22] and manganese complexes are influenced by counter-anions and non-coordinating ligand parts.[15] Certainly, the redox properties of metals show the major influence that was also proved by comparing superoxide scavenging reaction of Mn, Fe, Co and Ni complexes of the identical ligand (**7**). The highest activity of Fe was observed at that time (Fig 13).[53] Although, the series is not complete (missing data for homoleptic complex of Cu) it is clear that iron and copper have promising values at least among the SOD models (see also Fig 14).

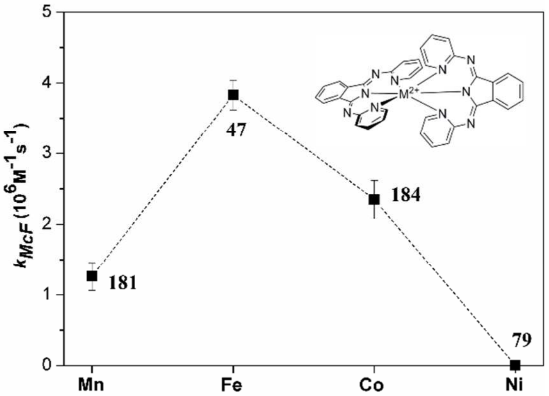

Fig. 13. Rate constants for the superoxide scavenging reaction of 1:2 ratio (metal-ligand) complexes of **7**.[53]

Figure 14 shows the k_{McF} rate constants plotted against the $E_{1/2}°'$ for all complexes that have been investigated as SOD models. A clear trend is observable in case of Cu and Fe while Mn and Co act differently. Redox potential values can be set where SOD activity is optimal. These are around the CuZnSOD redox couple (~ 0.06 V vs. Ag/AgCl in 1 M KCl at pH 7.5 in HEPES buffer)[128] and above the $O_2/O_2^{\bullet-}$ potential (– 0.40 V vs. SCE – saturated calomel electrode).[129-131]

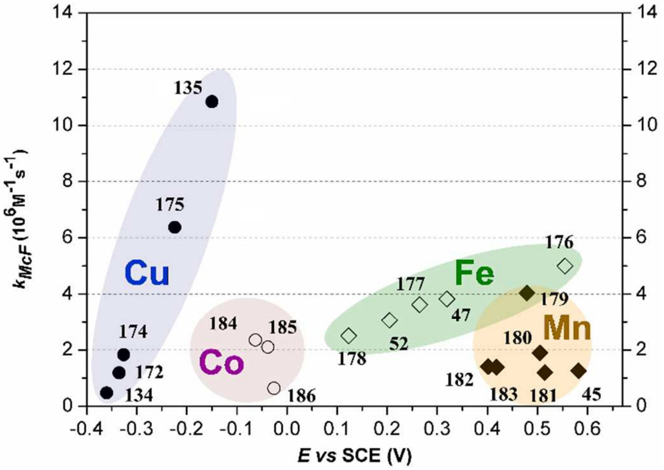

Fig. 14. pH = 7.6, 25°C, 0.1 M HEPES buffer. $O_2^{\bullet-}$ source: xanthin/Xanthin oxidase

The N-donor coordination sphere built by BIIs is an accurate model environment of CuZnSOD's copper, where three histidine ligands surround that part of the active center. As it was mentioned earlier cobalamins[127] can approach SOD activity implying to further ligand effects that have to be taken into consideration for future modelling studies.

4.1.4. Catechol oxidase mimics

The oxidation of *ortho*-diphenols to *ortho*-benzoquinones is among the first steps in melanin synthesis. The group of these molecules are responsible for tan skin. The initial part of the biosynthesis is enzyme catalyzed.[132] There are two enzymes involved in this transformation: the catechol oxidase and tyrosinase. The latter possesses an extra function that is the monooxidation of phenols. A binuclear copper(II) center is attributed to the specific activity where cores are connected by a double oxo-bridge in μ-η^2:η^2 form. A cyclic pathway between dezoxy (inactive) and oxy (active) form of the enzyme is the driving force of catechol oxidation as it is depicted in Scheme 7.

Model experiments are usually carried out with 3,5-di-*tert*-butylcatechol to avoid dimerization. Products are 3,5-di-*tert*-butyl-1,2-benzoquinone (3,5-DTBQ) and H_2O_2. As it is expected from model systems the activities are several magnitudes lower compared to the enzyme. The slow transformation is fortunate for reaction kinetic observations. The k_{cat}/K_M and TON values of Table 15 give the general information on substrate conversion during time unit. Turnover rate differences show that binuclear PAP complex have better mimicking properties at the same time mononuclear BIIs are more suitable for the investigations of influential factors. The only binuclear copper complex (**126**) is the most accurate catecholase structural model. The Cu-Cu distance is 3.274 Å that makes catechol coordination possible.

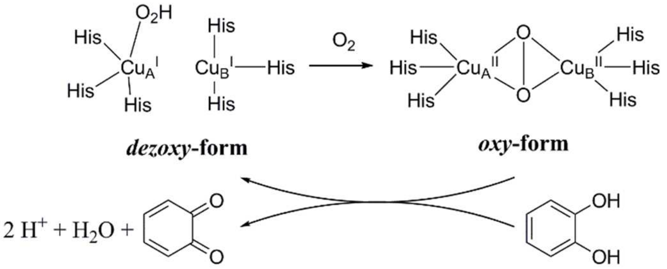

Scheme 7. The proposed catalytic cycle of catechol oxidase model reactions

Table 15
Catecholase model isoindoline complexes

Ligand	Complex	TON (h^{-1})	k_{cat}/K_M ($M^{-1}s^{-1}$)	Ref.
-	*Catechol oxidase from I. batatas*	-	8250	[133]
12	$[Mn_2(6'Me_2PAP)_2Cl_4]$ (**187**)	167.9	7.25	[99]
12	$[Mn(6'Me_2indH)(H_2O)_2(CH_3CN)](ClO_4)_2$ (**188**)	48.8	1.07	[16]
7NMe	$[Cu^I(Me_2ind)I_2]$ (**189**)	65.0	67.40	[33]
8	$[Cu_2^{II}(4'Me\text{-}ind)_2(MeOH)(\mu\text{-}OH)]ClO_4$ MeOH (**126**)	-	0.749	[91]
11	$[Cu(3'MePyOIND)_2]$ (**142**)	21.5	23.37	[23]

According to the enzymatic met (native) and oxy form the ideal distance has to be between 2.9 Å and 3.8 Å. The enzyme like behavior of models is attributed to the binuclear cores (with the appropriate distances) and to the presence of enzyme-like N-donor environment (Fig. 15).

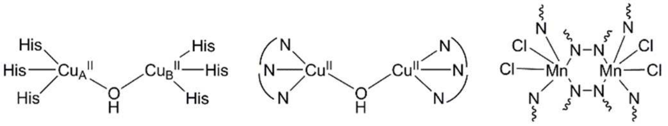

Fig. 15. Catechol oxidase active site (left), the coordination environment of $[Cu^{II}_2(4'Me\text{-}ind)_2(MeOH)(\mu\text{-}OH)]ClO_4$ MeOH (**126**) (middle)[91] and the proposed structure of $[Mn_2(6'Me_2PAP)_2Cl_4]$ (**187**) (right)[99]

Observations from the kinetic experiments imply to a biocatalytic circle where a ternary complex of dioxygen, substrate and catalyst is involved, furthermore bases and electron donating potential of the substrate have an effect on the mechanism. Basicity is considerable from both catalyst and external side as the prior deprotonation of the catechol is required for the activation of the "dezoxy form" of the catalyst.[16,23]

4.1.5. Catechol dioxygenase and other oxygenase properties

Nature's way to eliminate some environmentally harmful aromatics and polyphenols is owing to the oxygenase, dioxygenase family. In the aromatic bond cleavage process dioxygen is greatly involved. The reaction products are usually water-soluble aliphatic compounds that are easily utilized by any life form. Catechol dioxygenases are nonheme iron-dependent enzymes that are capable of such conversions. Depending on the site of action there are intra- and extradiol cleaving enzymes (breaking aromatic bonds between adjacent OH groups and outside of that respectively). A series of Fe-aroBIIs with the general formula of $Fe^{III}Cl_2(L)$ have been found to mimic intradiol-cleaving catechol 1,2-dioxygenase enzymes. Some electrochemical data showed that by using ligand varieties the Lewis acidity of the iron(III) center can be fine-tuned. This has a straight effect on the oxidation potentials ($E^{\circ\prime}_{pa}$) that determine the k values of dioxygenation reactions. Based on the kinetic data two possible pathways have been suggested for the mechanism explaining the role of dioxygen and steric effects (Scheme 8).[65]

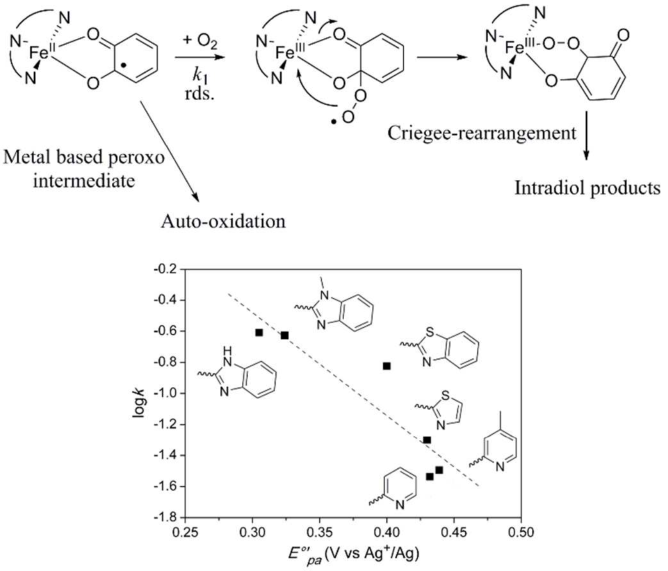

Scheme 8. The proposed mechanism of catechol 1,2-dioxygenase model reactions (top) and the effect of fine-tuning on the k reaction rate (bottom)[65]

The reaction mechanism of catechol dioxygenase mimics hypothesize certain active iron-oxygen species that can materialize primarily from iron(III). In the most recent works of our group we had special attention on stable 1,2-peroxodiiron(III) intermediates.[34,68] These species have been identified in several industrially promising enzymes (eg. soluble methane monooxygenase, ribonucleotide reductase or desaturases) by Raman and EXAFS spectroscopy,[134,135] furthermore by characteristic UV-Vis vibrations at 600-750 nm closer to the near-infrared region. Oxidation reactions of thioanisoles and benzyl alcohols have been investigated in the presence of H_2O_2 using mild reaction conditions aiming for selectively oxidized products. The work presented in these papers contains proofs of a metal-based oxidant with the clear exclusion of hydroxyl radicals. Reactions with para-substituted reagents showed changes in oxidation rate as a function of the nature of the para substituent. The negative Hammett ρ values were indicative of an electrophilic oxidant, furthermore KIE (kinetic isotope effect) supported the theory about the lack of radical involvement. Results are a part of a continuous research on the role of metal-based oxidants in non-heme diiron enzymes.

4.2. Catalysis; chemical, quantum chemical and biological applications

AroBII ligands possess undoubtedly perfect properties for complex formation. Structural properties, coordination modes and unexpected molecular configurations are presented by the majority of scientific papers. Better understanding in basic features leads to new ideas for applications that show a growing tendency year by year.

4.2.1. C-H and C-C bond activation

Predominantly intramolecular C(sp^3)–H bond activation has been observed in a greater number of palladium complexes with aroBII.[39-41,86] It was found that an excess of palladium salt changes the coordination sphere and flips one arm on BII by creating an organometallic compound. The irregular behavior is attributed to steric factors and the stability of Pd–C bond.

Palladacycles are known with unsyBIIs as well.[136,137] C$_{aryl}$–H bond activation was observed in this case.

Catalytic hydrogenation with palladium has been carried out with more efficacy on aliphatic olefins.[18] It is notable that the catalyst could be reused in several cycles.

4.2.2. Oxidation, peroxidation and epoxidation

It has been general knowledge for decades that certain transition metals tend to form metal-oxo species that are strong oxidizing agents even at mild conditions (room temperature, atmospheric pressure, no co-catalyst added). The first steps towards perfect homogenous catalysts required additional reactants. Ruthenium complexes of BIIs were found to be able to catalyze alcohol oxidation in the presence of bases with good coordinating ability.[74] By the right metal ion choice stable hydoperoxo intermediates have been characterized with cobalt (**67**) and used in hydrocarbon hydroxylation, oxidation.[60,76]

Multiple papers from L. H. Gade's group describe C=C bond activation. The peroxylation of cyclohexene to *tert*-butylperoxy-3-cyclohexene has been tested with copper, cobalt and iron complexes.[61,88] Selectivity towards the desired product was reported to be outstanding. Using highly reactive oxaziridine type oxidizing agents even epoxidation products have been detected from a great number of olefins by iridium-aroBIIs (Scheme 9).[78]

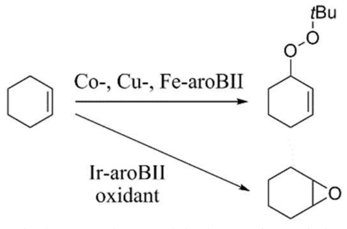

Scheme 9. Peroxylation and epoxidation of cyclohexene with aroBII complexes

Cobalt(III)–alkylperoxy complexes can be activated by high energy light irradiation. Oxidation products of alkanes or alkenes are alkylperoxides or ketones/alcohols depending on the presence of inert atmosphere.[138]

4.2.3. Photoactivity and optical properties

The extended aromatic structure of BIIs is an advantageous environment for dynamic intra- and intermolecular processes that determine photophysical properties. Hanson et al. presented an extensive study on fine-tuned BII derivatives with keto-enol tautomerism. The ligands are capable of proton-transfer between the OH group and NH group on the isoindole core. Quantum efficiencies are up to 45%.[54]

Quantum yields dramatically change when luminescence of complexes is investigated. It dropped below 5 % when platinum or rare earth metals have been measured.[19,32,46]

Specific optical properties have a wide range of applications in modern electronic devices. Crystallographic direction dependent refractive index (birefringence) has been determined for a few aroBII ligands. These values describe the 3D structure of a crystalline material giving information on anisotropic polarizability or supramolecular orientation, *etc.*[139]

4.2.4. Chiral hydrosilylation, cyclopropanation, fluorination

Enantioselective behavior of Fe and Co chiBIIs has been tested in asymmetric hydrosilylation and cyclopropanation (Scheme 10). Usually, chiral pincer type ligands perform poorly in enantioselective catalysis but with careful design on the stereodirecting unit and with protection from backside attack to the metal center remarkable results have been obtained.[13,37] The variety of asymmetric test reactions has been extended to the fluorination of oxindoles and β-ketoesters with Ni-chiBIIs.[36]

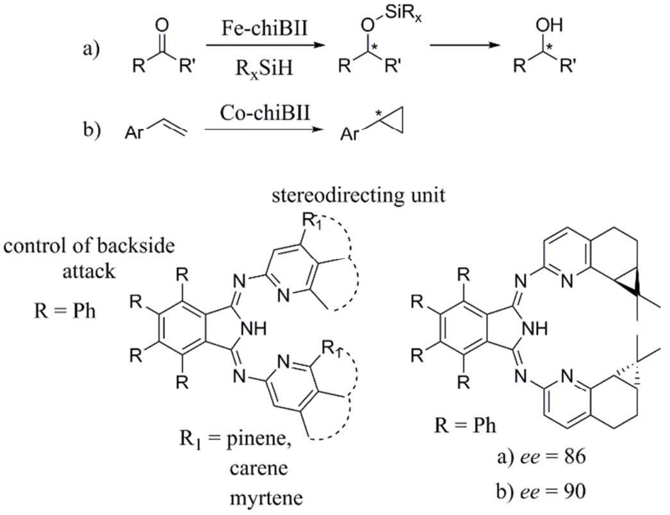

Scheme 10. Asymmetric hydrosilylation and cyclopropanation reactions catalysed by chiBII complexes

4.2.5. DNA interaction, antiproliferative activity

Complex interaction with DNA is studied for biotechnological purposes. The development of new therapeutic agents, or non-radioactive DNA probes is the aim of these studies. A unique interaction has been expected from octahedral Co(BPI)$_2$ complexes by excluding specific binging site targeting. It was found that electrostatic forces determine DNA interaction and they are stronger in Co(III) complexes.[62]

UnsyBIIs have already been discussed (see above) in their active palladacycle form and as bidentate N-donor ligands. Recently, antiproliferative activity has been tested too on five human tumor cell lines. The results serve as guideline for future development of bioactive isoindoline derivatives.[10]

5. Perspectives

The approximately six decades long history of bis-iminoisoindoline derivatives and complexes led to numerous discoveries in their chemistry and biochemistry. Now, with precise insight into all structural features and with all the improved techniques in synthesis there is a great opportunity to further exploit their capabilities. There is just and endless possibility to attach various sidearms on DII cores that control enantioselective, anionic and coordinative behavior. Fine-tuning of these ligands is simply prominent. Photophysical properties both by crystallographic means and ligand based should be taken into consideration for research directions. In catalysis, the pincer-type coordination defines two major trends. 1:1 complexes are successfully applied on several fields due to the accessibility of the metal center while octahedral 2:1 complexes are limited to specific interactions. The greatly promising achievements in enzyme mimics have significance in modern drug development.

Acknowledgements

Financial support of the Hungarian National Research Fund (OTKA K108489), TÁMOP-4.2.2.A-11/1/KONV-2012-0071, TÁMOP-4.2.2/B-10/1-2010-0025, and COST CM1003 are gratefully acknowledged.

Notes and references

Department of Chemistry, University of Pannonia, 8201 Veszprém, Hungary
E-mail: kaizer@almos.vein.hu
See DOI: 10.1039/b000000x/

1 J. A. Elvidge and R. P. Linstead, *J. Chem. Soc.*, 1953, 5000.
2 P. F. Clark, J. A. Elvidge and R. P. Linstead, *J. Chem. Soc.*, 1953, 3593.
3 W. O. Siegl, *Inorg. Chim. Acta*, 1977, **25**, L65.
4 R. R. Gagné, R. S. Gall, G. S. Lisensky, R. E. Marsh and L. M. Speltz, *Inorg. Chem.*, 1979, **18**, 771.
5 R. R. Gagné, W. A. Marritt, D. N. Marks and W. O. Siegl, *Inorg. Chem.*, 1981, **20**, 3260.
6 A. W. Addison, P. J. Burke and K. Henrick, *Inorg. Chem.*, 1982, **21**, 60.
7 W. O. Siegl, *J. Org. Chem.*, 1977, **42**, 1872.
8 G. de la Torre, P. Vázquez, F. Agulló-López and T. Torres, *Chem. Rev.*, 2004, **104**, 3723.
9 H. Alivan and J. E. Lier, Porphyrins and Phthalocyanines as Photosensitizers and Radiosensitizers. In *Handbook of Porphyrin Science*; K. M. Kadish, K. M. Smith and R. Guilard, Eds.; World Scientific Publishing: Singapore, 2010, **Vol 4.**, pp 1–99.
10 I. Sović, V. Stilinović, B. Kaitner, S. Kraljević-Pavelić, M. Bujak, K. Čuljak, P. Novak and G. Karminski-Zamola, *J. Mol. Struct.*, 2011, **1006**, 259.
11 G. Cignarella and P. Sanna, *J. Med. Chem.*, 1981, **24**, 1003.
12 S. Klutchko, C. J. Blankley, R. W. Fleming, J. M. Hinkley, A. E. Werner, I. Nordin, A. Holmes, M. L. Hoefle, D. M. Cohen, A. D. Essenburg and H. R. Kaplan, *J. Med. Chem.*, 1986, **29**, 1953.
13 B. K. Langlotz, H. Wadepohl and L. H. Gade, *Angew. Chem. Int. Ed.*, 2008, **47**, 4670.
14 L. K. Thompson, V. T. Chacko, J. A. Elvidge, A. B. P. Lever and R. V. Parish, *Can. J. Chem.*, 1969, **47**, 4141.
15 J. S. Pap, B. Kripli, T. Váradi, M. Giorgi, J. Kaizer and G. Speier, *J. Inorg. Biochem.*, 2011, **105**, 911.
16 J. Kaizer, G. Barath, R. Csonka, G. Speier, L. Korecz, A. Rockenbauer and L. Párkányi, *J. Inorg. Biochem.*, 2008, **102**, 773.
17 J. Kaizer, T. Csay, P. Kővári, G. Speier and L. Párkányi, *J. Mol. Catal. A: Chem.*, 2008, **280**, 203.
18 B. Siggelkow, M. B. Meder, C. H. Galka and L. H. Gade, *Eur. J. Inorg. Chem.*, 2004, 3424.
19 H-M. Wen, Y-H. Wu, Y. Fan, L-Y. Zhang, C-N. Chen and Z-N. Chen, *Inorg. Chem.*, 2010, **49**, 2210.
20 I-S. Tamgho, J. T. Engle and C. J. Ziegler, *Tetrahedron Lett.*, 2013, **54**, 6114.
21 P. J. Domaille, R. L. Harlow, S. D. Ittel and W. G. Peet, *Inorg. Chem.*, 1983, **22**, 3944.
22 B. Kripli, G. Baráth, É. Balogh-Hergovich, M. Giorgi, A. J. Simaan, L. Párkányi, J. S. Pap, J. Kaizer and G. Speier, *Inorg. Chem. Commun.*, 2011, **14**, 205.
23 J. Kaizer, T. Csay, G. Speier and M. Giorgi, *J. Mol. Catal. A: Chem.*, 2010, **329**, 71.
24 C. G. Claessens, U. Hahn and T. Torres, *Chem. Rec.*, 2008, **8**, 75.
25 A. B. Sorokin, *Chem. Rev.*, 2013, **113**, 8152.
26 P. F. Clark, J. A. Elvidge and J. H. Golden, *J. Chem. Soc.*, 1956, 4135.
27 H. A. Luts, *J. Pharm. Sci.*, 1969, **58**, 496.
28 R. Sato, T. Senzaki, Y. Shikazaki, T. Goto and M. Saito, *Chem. Lett.*, 1984, 1423.
29 R. Sato, M. Nakayama, Y. Yuzawa, T. Goto and M. Saito, *Chem. Lett.*, 1985, 1887.
30 V. V. Negrebetskii, O. V. Balitskaya and M. Y. Kornilov, *J. Gen. Chem., USSR (Engl. Transl.)*, 1983, **53**, 2320.
31 M. N. Bochkarev, T. V. Balashova, A. A. Maleev, I. I. Pestova, G. K. Fukin, E. V. Baranov and Y. A. Kurskii, *Russ. Chem. Bull. Int. Ed.*, 2008, **57**, 2162.
32 A. A. Maleev, T. V. Balashova, G. K. Fukin, M. A. Katkova, M. A. Lopatin and M. N. Bochkarev, *Polyhedron*, 2010, **29**, 10.
33 Á. Kupán, J. Kaizer, G. Speier, M. Giorgi, M. Réglier and F. Pollreisz, *J. Inorg. Biochem.*, 2009, **103**, 389.
34 J. S. Pap, M. A. Cranswick, É. Balogh-Hergovich, G. Baráth, M. Giorgi, G. T. Rohde, J. Kaizer, G. Speier and L. Que Jr., Eur. *J. Inorg. Chem.*, 2013, 3858.
35 N. C. Fletcher, F. R. Keene, M. Ziegler, H. Stoeckli-Evans, H. Viebrock and A. von Zelewsky, *Helv. Chim. Acta*, 1996, **79**, 1192.
36 Q-H. Dang, H. Wadepohl and L. H. Gade, *Chem. Eur. J.*, 2011, **17**, 14922.
37 D. C. Sauer, H. Wadepohl and L. H. Gade, *Inorg. Chem.*, 2012, **51**, 12948.
38 M. Bröring and C. Kleeberg, *Inorg. Chim. Acta*, 2009, **362**, 1065.
39 B. L. Dietrich, J. Egbert, A. M. Morris and M. Wicholas, *Inorg. Chem.*, 2005, **44**, 6476.
40 M. Bröring and C. Kleeberg, *Dalton Trans.*, 2007, 1101.
41 M. Bröring, C. Kleeberg and E. C. Tejero, *Eur. J. Inorg. Chem.*, 2007, 3208.

42 M. Bröring, C. Kleeberg and S. Köhler, *Inorg. Chem.*, 2008, **47**, 6404.
43 C. Kleeberg and M. Bröring, *Polyhedron*, 2010, **29**, 507.
44 A. W. Addison and T. N. Rao, *J. Chem. Soc. Dalton Trans.*, 1984, 1349.
45 M-A. Munoz-Hernandez, T. S. Keizer, P. Wei, S. Parkin and D. A. Atwood, *Inorg. Chem.*, 2001, **40**, 6782.
46 J. S. Pap, B. Kripli, V. Bányai, M. Giorgi, L. Korecz, T. Gajda, D. Árus, J. Kaizer and G. Speier, *Inorg. Chim. Acta*, 2011, **376**, 158.
47 J. S. Pap, V. Bányai, D. S. Szilvási, J. Kaizer, G. Speier and M. Giorgi, *Inorg. Chem. Comm.*, 2011, **14**, 1767.
48 É. Balogh-Hergovich, G. Speier, M. Réglier, M. Giorgi, E. Kuzmann and A. Vértes, *Inorg. Chem. Commun.*, 2005, **8**, 457.
49 J. Kaizer, G. Baráth, G. Speier, M. Réglier and M. Giorgi, *Inorg. Chem. Commun.*, 2007, **10**, 292.
50 J. Kaizer, B. Kripli, G. Speier and L. Párkányi, *Polyhedron*, 2009, **28**, 933.
51 J. S. Pap, M. Giorgi, J. Kaizer and G. Speier, *Inorg. Chem. Commun.*, 2013, **27**, 152.
52 U.S. Pat. 4 568 769 to Sumitomo (A. Yashima, T. Matsuda, T. Sato, M. Takahashi and K. Sakai), 1986.
53 J. S. Pap, B. Kripli, M. Giorgi, J. Kaizer and G. Speier, *Trans. Met. Chem.*, 2011, **36**, 481.
54 K. Hanson, N. Patel, M. T. Whited, P. I. Djurovich and M. E. Thompson, *Org. Lett.*, 2011, **13**, 1598.
55 D. M. Baird, R. Hassan and W. K. Kim, *Inorg. Chim. Acta*, 1987, **130**, 39.
56 D. M. Baird and K. Y. Shih, *Polyhedron*, 1989, **8**, 2359.
57 G. E. O. Borgstahl, H. E. Parge, M. J. Hickey, W. F. Beyer Jr., R. A. Hallewell and J. A. Tainer, *Cell*, 1992, **71**, 107.
58 P. Chelikani, I. Fita and P. C. Loewen, *Cell. Mol. Life Sci.*, 2004, **61**, 192.
59 G. Martić, J. T. Engle and C. J. Ziegler, *Inorg. Chem. Commun.*, 2011, **14**, 1749.
60 L. Saussine, E. Brazil, A. Robine, H. Mimoun, J. Fischer and R. Weiss, *J. Am. Chem. Soc.*, 1985, **107**, 3534.
61 M. B. Meder, B. A. Siggelkow and L. H. Gade, *Z. Anorg. Allg. Chem.*, 2004, **630**, 1962.
62 P. T. Selvi, H. Stoeckli-Evans and M. Palaniandavar, *J. Inorg. Biochem.*, 2005, **99**, 2110.
63 É. Balogh-Hergovich, G. Speier, M. Réglier, M. Giorgi, E. Kuzmann and A. Vértes, *Eur. J. Inorg. Chem.*, 2003, 1735.
64 É. Balogh-Hergovich, G. Speier, B. Tapodi, M. Réglier and M. Giorgi, *Z. Kristallogr.*, 1999, **214**, 579.
65 T. Váradi, J. S. Pap, M. Giorgi, L. Párkányi, T. Csay, G. Speier and J. Kaizer, *Inorg. Chem.*, 2013, **52**, 1559.
66 J. T. Engle, G. Martić and C. J. Ziegler, *Macroheterocycles*, 2013, **6**, 353.
67 M. Szávuly, R. Csonka, G. Speier, R. Barabás, M. Giorgi and J. Kaizer, *J. Mol. Catal. A: Chem.*, 2014, **392**, 120.
68 M. Szávuly, S. D. Szilvási, R. Csonka, D. Klesitz, G. Speier, M. Giorgi and J. Kaizer, *J. Mol. Catal. A: Chem.*, 2014, **393**, 317.
69 M. Kruck, D. C. Sauer, M. Enders, H. Wadepohl and L. H. Gade, *Dalton Trans.*, 2011, **40**, 10406.
70 D. C. Sauer, M. Kruck, H. Wadepohl, M. Enders and L. H. Gade, *Organometallics*, 2013, **32**, 885.
71 M. A. Robinson, S. I. Trotz and T. J. Hurley, *Inorg. Chem.*, 1967, **6**, 392.
72 T. S. Pitchumony and H. Stoeckli-Evans, *Acta Cryst.*, 2005, **E61**, 69.
73 D. N. Marks, W. O. Siegl and R. R. Gagné, *Inorg. Chem.*, 1982, **21**, 3140.
74 R. R. Gagné and D. N. Marks, *Inorg. Chem.*, 1984, **23**, 65.
75 K-N. T. Tseng, J. W. Kampf and N. K. Szymczak, *Organometallics*, 2013, **32**, 2046.
76 C. A. Tolman, J. D. Druliner, P. J. Krusic, M. J. Nappa, W. C. Seidel, I. D. Williams and S. D. Ittel, *J .Mol. Catal.*, 1988, **48**, 129.
77 B. K. Langlotz, J. L. Fillol, J. H. Gross, H. Wadepohl and L. H. Gade, *Chem. Eur. J.*, 2008, **14**, 10267.
78 J. A. Camerano, C. Sämann, H. Wadepohl and L. H. Gade, *Organometallics*, 2011, **30**, 379.
79 W. O. Siegl, *J. Organomet. Chem.*, 1976, **107**, C27.
80 R. J. Letcher, W. Zhang, C. Bensimon and R. J. Crutchley, *Inorg. Chim. Acta*, 1993, **210**, 183.
81 M. Meder, C. H. Galka and L. H. Gade, *Monatsh. Chem.*, 2005, **136**, 1693.
82 M. Bröring, C. Kleeberg and A. Scheja, *Inorg. Chim. Acta*, 2011, **374**, 572.
83 M. Bröring and C. Kleeberg, *Z. Anorg. Allg. Chem.*, 2007, **633**, 2210.
84 M. Bröring and C. Kleeberg, *Z. Anorg. Allg. Chem.*, 2011, **637**, 1769.
85 M. Bröring and C. Kleeberg, *Inorg. Chim. Acta*, 2007, **360**, 3281.
86 M. Bröring and C. Kleeberg, *Chem. Commun.*, 2008, 2777.
87 H-M. Wen, Y-H. Wu, L-J. Xu, L-Y. Zhang, C-N. Chen and Z-N. Chen, *Dalton Trans.*, 2011, **40**, 6929.
88 M. B. Meder and L. H. Gade, *Eur. J. Inorg. Chem.*, 2004, 2716.
89 J. Kaizer, J. Pap, G. Speier, M. Réglier and M. Giorgi, *Trans. Met. Chem.*, 2004, **29**, 630.
90 D. M. Baird, W. P. Maehlmann, R. D. Bereman and P. Singh, *J. Coord. Chem.*, 1997, **42**, 107.
91 T. Csay, B. Kripli, M. Giorgi, J. Kaizer and G. Speier, *Inorg. Chem. Commun.*, 2010, **13**, 227.
92 O. P. Anderson, A. la Cour, A. Dodd, A. D. Garrett and M. Wicholas, *Inorg. Chem.*, 2003, **42**, 122.
93 D. C. Sauer and H. Wadepohl, *Polyhedron*, 2014, **81**, 180.
94 M. Wicholas, A. D. Garrett, M. Gleaves, A. M. Morris, M. Rehm, O. P. Anderson and A. la Cour, *Inorg. Chem.*, 2006, **45**, 5804.
95 J. L. Cryder, A. J. Killgore, C. Moore, J. A. Golen, A. L. Rheingold and C. J. A. Daley, *Dalton Trans.*, 2010, **39**, 10671.
96 M. Wicholas, B. L. Dietrich, O. P. Anderson and A. la Cour, *Acta Cryst.*, 2006, **E62**, m1689.
97 O. P. Anderson, A. la Cour, A. Berg, A. D. Garrett and M. Wicholas, *Inorg. Chem.*, 2003, **42**, 4513.
98 H. Irving and R. J. P. Williams, *J. Chem. Soc.*, 1953, 3192.
99 J. Kaizer, R. Csonka, G. Baráth and G. Speier, *Trans. Met. Chem.*, 2007, **32**, 1047.
100 G. Marongiu and E. C. Lingafelter, *Acta Cryst.*, 1982, **B38**, 620.
101 É. Balogh-Hergovich, G. Speier, M. Réglier, M. Giorgi, E. Kuzmann and A. Vértes, *Inorg. Chim. Acta*, 2004, **357**, 3689.
102 G. Bullock, A. Cook, A. Foster, L. Rosenberg and L. K. Thompson, *Inorg. Chim. Acta*, 1985, **103**, 207.
103 S. K. Mandal, L. K. Thompson and M. J. Newlands, *Inorg. Chim. Acta*, 1986, **122**, 199.

104 C. L. Sheppard, S. S. Tandon, L. K. Thompson, J. N. Bridson, D. O. Miller, M. Handa and F. Lloret, *Inorg. Chim. Acta*, 1996, **250**, 227.

105 L. K. Thompson, V. Niel, H. Grove, D. O. Miller, M. J. Newlands, P. H. Bird, W. A. Wickramasinghe and A. B. P. Lever, *Polyhedron*, 2004, **23**, 1175.

106 J. S. Pap, J. Kaizer, M. Giorgi and G. Speier, *Inorg. Chem. Commun.*, 2010, **13**, 1069.

107 M. Albrecht and G. van Koten, *Angew. Chem. Int. Ed.*, 2001, **40**, 3750.

108 A. W. Smith, A. Camara-Artigas, M. Wang, J. P. Allen and W. A. Francisco, *Biochemistry*, 2006, **45**, 4378.

109 L. Prati, M. Rossi and N. Ravasio, *J. Mol. Cat.*, 1992, **75**, 347.

110 C. E. Barry, P. G. Nayar and T. P. Begley, *Biochemistry*, 1989, **28**, 6323.

111 K. Anzai, K. Isono, K. Ohkuma and S. Suzuki, *J. Antibiotics Ser. A.*, 1960, **13**, 125.

112 L. I. Simándi, T. M. Barna, L. Korecz and A. Rockenbauer, *Tetrahedron Lett.*, 1993, **34**, 717.

113 T. M. Simándi, L. I. Simándi, M. Győr, A. Rockenbauer and Á. Gömöry, *Dalton Trans.*, 2004, 1056.

114 I. C. Szigyártó, T. M. Simándi, L. I. Simándi, L. Korecz and N. Nagy, *J. Mol. Catal. A: Chem.*, 2006, **251**, 270.

115 C. D. Putnam, A. S. Arvai, Y. Bourne and J. A. Tainer, *J. Mol. Biol.*, 2000, **296**, 295.

116 A. Sigel, H. Sigel and R. K. O. Sigel, *Metal Ions in Life Sciences, Volume 1. Neurodegenerative Diseases and Metal Ions*, John Wiley & Sons Ltd, 2006.

117 M. U. Triller, W-Y. Hsieh, V. L. Pecoraro, A. Rompel and B. Krebs, *Inorg. Chem.*, 2002, **41**, 5544.

118 E. J. Larson and V. L. Pecoraro, *J. Am. Chem. Soc.*, 1991, **113**, 7809.

119 A. E. M. Boelrijk and G. C. Dismukes, *Inorg. Chem.*, 2000, **39**, 3020.

120 T. Csay, J. Kaizer and G. Speier, *React. Kinet. Catal. Lett.*, 2009, **96**, 35.

121 B. L. Stoddard, P. L. Howell, D. Ringe and G. A. Petsko, *Biochemistry*, 1990, **29**, 8885.

122 L. C. Tabares, J. Gätjens and S. Un, *Biochim. Biophys. Acta*, 2010, **1804**, 308.

123 J. A. Tainer, E. D. Getzoff, J. S. Richardson and D. C. Richardson, *Nature*, 1983, *306*, 284.

124 D. P. Barondeau, C. J. Kassmann, C. K. Burns, J. A. Tainer and E. D. Getzoff, *Biochemistry*, 2004, **43**, 8038.

125 J. M. McCord and I. Fridovich, *J. Biol. Chem.*, 1969, **244**, 6049.

126 D. P. Riley, *Chem. Rev.*, 1999, **99**, 2573.

127 E. Suarez-Moreira, J. Yun, C. S. Birch, J. H. H. Williams, A. McCaddon and N. E. Brasch, *J. Am. Chem. Soc.*, 2009, **131**, 15078.

128 B. Ge, F. W. Scheller and F. Lisdat, *Biosens. Bioelectron.*, 2003, **18**, 295.

129 W. H. Koppenol, F. Levine, T. L. Hatmaker, J. Epp and J. D. Rush, *Arch. Biochem. Biophys.*, 1986, **251**, 594.

130 P. M. Wood, *Biochem. J.*, 1988, **253**, 287.

131 I. Batinic-Haberle, I. Spasojevic, R. D. Stevens, P. Hambright, P. Neta, A. Okado-Matsumoto and I. Fridovich, *Dalton Trans.*, 2004, 1696.

132 C. Eicken, B. Krebs and J. C. Sacchettini, *Curr. Opin. Struct. Biol.*, 1999, **9**, 677.

133 S. J. Smith, C. J. Noble, R. C. Palmer, G. R. Hanson, G. Schenk, L. R. Gahan and M. J. Riley, *J. Biol. Inorg. Chem.*, 2008, **13**, 499.

134 A. J. Skulan, T. C. Brunold, J. Baldwin, L. Saleh, J. M. Bollinger, Jr. and E. I. Solomon, *J. Am. Chem. Soc.*, 2004, **126**, 8842.

135 M. Srnec, T. A. Rokob, J. K. Schwartz, Y. Kwak, L. Rulisek and E. I. Solomon, *Inorg. Chem.*, 2012, **51**, 2806.

136 J. M. Chitanda, D. E. Prokopchuk, J. W. Quail and S. R. Foley, *Dalton Trans.*, 2008, 6023.

137 J. M. Chitanda, S-C. Wu, J. W. Quail and S. R. Foley, *Inorg. Chim. Acta*, 2011, **379**, 122.

138 E. T. Farinas, C. V. Nguyen and P. K. Mascharak, *Inorg. Chim. Acta*, 1997, **263**, 17.

139 E. W. Y. Wong, J. S. Ovens and D. B. Leznoff, *Chem. Eur. J.*, 2012, **18**, 6781.